Journal of Sea Research 191 (2023) 102309

Contents lists available at ScienceDirect

Journal of Sea Research

journal homepage: www.elsevier.com/locate/seares

Recovery patterns of the coral microbiome after relief of algal contact

Fleur C. van Duyl [a,*], Judith D.L. van Bleijswijk [a], Cornelia Wuchter [b], Harry J. Witte [a], Marco J.L. Coolen [b], Rolf P.M. Bak [a], Julia C. Engelmann [a], Maggy M. Nugues [c,d]

[a] Marine Microbiology and Biogeochemistry, NIOZ Royal Netherlands Institute for Sea Research, PO Box 59, 1790AB Texel, the Netherlands
[b] Curtin University, School of Earth and Planetary Sciences, WA Organic and Isotope Geochemistry Centre (WA-OIGC), Bentley, WA 6102, Australia
[c] EPHE-UPVD-CNRS, USR 3278 CRIOBE, PSL Research University, 66860 Perpignan, France
[d] Laboratoire d'Excellence "CORAIL", 98729 Moorea, French Polynesia

ARTICLE INFO

Keywords:
Coral-algal interaction
Coral microbiome dynamics
Recovery

ABSTRACT

Interactions between macroalgae and corals are omnipresent on eutrophied and overfished reefs worldwide. Contact with macroalgae can disrupt corals and their microbiomes through diverse mechanisms, including shading, abrasion, and the release of algal exudates. However, changes in the coral microbiome after algal contact ceases have not been studied. We investigated the recovery of the microbiome of massive reef-building *Porites* corals following experimental removal of the overgrowing green macroalga *Halimeda macrophysa*. We followed changes in the microbiome of macroalgal-removed and adjacent healthy-looking tissue of coral colonies over 40 days. Coral tissue was predominantly bleached underneath the macroalgae but regained almost its full pigmentation by day 40. Despite this recovery in pigmentation, the bacterial microbiome of macroalgal-removed coral tissue did not return to that of adjacent healthy-looking tissue (control). Overall, macroalgal contact led to the suppression of Gammaproteobacteria and increased diversity and dominance of Alphaproteobacteria, a shift that persevered for 40 days after algal removal. Causal effect analysis showed a positive effect of influential OTUs in healthy-looking tissue assigned to Gammaproteobacteria and Bacteroidia on the relative abundance of other OTUs within these classes. The effect of influential OTUs assigned to Alphaproteobacteria in macroalgal-removed tissue on the relative abundance of other OTUs was more diverse. Despite the high heterogeneity of coral microbiomes, differences in the relative abundance of main bacterial classes and orders between control/healthy and macroalgal-removed tissue showed temporal patterns. Differences in the Alpha-, Gamma-, Deltaproteobacteria and Bacteroidia between control/healthy and macroalgal-removed tissue increased after cessation of macroalga contact and stabilized or declined towards day 40. Acidimicrobiia, Deltaproteobacteria, Rhodospirillales and Rhodovibrionales returned to average relative abundances in the adjacent control/healthy tissue after 40 days. Nevertheless, Rhizobiales and Rhodobacterales (Alphaproteobacteria) still dominated the macroalgal-removed microbiome on day 40. We conclude that macroalgal overgrowth induces changes in the coral microbiome, and that algal removal did not lead to full recovery of the microbiome in 40 days. Return of pigmentation and distinct shifts in bacterial groups over time appear a possible pathway to the recovery of the coral microbiome after macroalgal removal.

1. Introduction

On coral reefs worldwide, benthic algae often increase at the expense of stony corals. This replacement is a consequence of changing environmental conditions on reefs favoring the growth of benthic algae over that of scleractinian corals (McCook et al., 2001). Enhanced nutrient supply, low grazing pressure on benthic algae, and decline of coral cover promote the proliferation of macroalgae on coral reefs (De Bakker et al., 2017; Jackson et al., 2014). Consequently, the frequency of interactions between macroalgae and corals increases. Various macroalgal species interacting with adjacent corals induce coral bleaching (loss of photosynthetic algal endosymbionts) and hypoxia in the contact zone (Haas et al., 2013; Titlyanov et al., 2007; Wangpraseurt et al., 2012). Coral-algal interactions often lead to the inhibition of coral growth and mortality of corals, perpetuating algal-dominance states (Titlyanov et al., 2007; Vega Thurber et al., 2012). However, the mechanisms underlying

* Corresponding author.
E-mail address: Fleur.van.Duyl@nioz.nl (F.C. van Duyl).

https://doi.org/10.1016/j.seares.2022.102309
Received 11 March 2022; Received in revised form 18 November 2022; Accepted 21 November 2022
Available online 5 December 2022

coral-algal interactions are still poorly understood (Clements et al., 2018). Macroalgae can affect coral health through several mechanisms, including shading, abrading/smothering coral tissue, and release of chemical and microbial compounds (Barott and Rohwer, 2012; Clements et al., 2020). In addition, coral-algal interactions can affect the coral microbiome, with algal-derived allelochemicals altering the composition and abundance of coral-associated microorganisms (Barott et al., 2012; Morrow et al., 2011; Rasher and Hay, 2010; Smith et al., 2006). Algae can also represent reservoirs for pathogens, which may cause diseases in stressed corals (Nugues et al., 2004; Sweet et al., 2013). Hence, microbes play a pivotal role in the dynamics of coral-algal interactions.

Corals harbor a diverse and often species-specific community of microorganisms (Bourne et al., 2016; Mouchka et al., 2010). The coral microbial community is distinct from that in the water column, whereas the community in the coral surface mucus layer is more closely associated with the surrounding water than with the coral tissue (Bourne and Munn, 2005; Hernandez-Agreda et al., 2018). The microbial communities associated with coral mucus and tissue, are considered beneficial to the health and survival of the coral holobiont (Krediet et al., 2013; Morrow et al., 2013). For example, mucus layer microbes protect corals from invading pathogens (Ritchie and Smith, 2004). However, little is known about the ecological mechanisms that govern the coral microbiome (Krediet et al., 2013; Shearer et al., 2012). Benthic macroalgae harbor a distinct and even more diverse microbial community than corals (Barott et al., 2011). In contact with macroalgae, coral-associated microbial communities shift towards bacterial taxa present in the algae or in water (Morrow et al., 2013; Vega Thurber et al., 2012). Shifts in coral microbial composition often correlate with signs of disease and/or bleaching, supporting the link between microbes and coral health (Boilard et al., 2020; Bourne et al., 2008; Mao-Jones et al., 2010; Rosenberg et al., 2009). In coral bleaching caused by heat stress, the resident microbial community can be replaced by pathogenic microbes (McDevitt-Irwin et al., 2017; Vega Thurber et al., 2009). Ongoing characterizations of microbiomes in stressed versus unstressed corals suggest that corals can shape their microbiome and core community associated with coral fitness characterized by specific taxa and functions (Ainsworth et al., 2015; Krediet et al., 2013; Voolstra and Ziegler, 2020).

Assessing post-disturbance microbial changes over time will contribute to better understanding of the role that microbial communities play in coral holobionts. For example, distinct shifts in the microbial community of the coral *Acropora millepora* occurred during bleaching events, with returns to the pre-stress microbial community after 2–3 months (Bourne et al., 2008). A partial return to the native microbial community after an ex situ treatment of the coral *Acropora muricata* with an antibiotic was achieved in 4 days (Sweet et al., 2011). Corals can also alter the structure of their native microbial community to adapt to changing environmental conditions (Ceh et al., 2011; Rosenberg et al., 2007; Ziegler et al., 2019). There may be a dynamic relationship between coral-associated microorganisms and their host in which the coral regulates the return to, or a change towards, a particular microbial community, which might be beneficial for its health (Bourne et al., 2016; Kvennefors et al., 2011; Maher et al., 2020; Peixoto et al., 2017; Ritchie, 2006; Rosenberg et al., 2007).

This study investigated the change in the coral microbiome following the experimental removal of overgrowing macroalgae on corals at Derawan Island, East Kalimantan, Indonesia. We chose the naturally co-occurring green macroalga *Halimeda macrophysa* and the massive *Porites* coral for this experiment because both were abundant in the backreef system of the island, with *H. macrophysa* frequently overgrowing massive *Porites* corals and causing the coral tissue to bleach underneath. Our aims were: (a) to assess the microbial community composition in the bleached coral after removal of overgrowing macroalgae and compare it with the microbiome on a visually unstressed part of the same coral colony, and (b) to follow the temporal changes in the microbiome of stressed tissue and compare it with unstressed tissue after removal of the macroalgae.

2. Materials and methods

2.1. Study site, field surveys and time-series experiments

Our study was carried out in Indonesia and was facilitated by the Research Centre of Oceanography (LIPI). Fieldwork was performed between October–December 2008 and February 2010 at 5–8 m depth on the back reef at Coral Garden (02° 17.641′N, 118° 15.712′ E) close to Derawan, a small island located on the shelf edge 20 km off the east coast of Kalimantan (Fig. 1). The island is exposed to the outflow of the Berau river whose discharge of total suspended solids increased since 1979 (Parwati et al., 2013). The reef ecosystem has experienced a decrease in coral cover with subsequent replacement by benthic algae due to heavy sedimentation, disease and an outbreak of the predatory sea star *Acanthaster planci* (Nugues and Bak, 2009).

Field surveys were conducted in 2010 to describe the cover and interaction between massive *Porites* and *Halimeda macrophysa*. The benthos was surveyed by photographing 20 1 × 1 m quadrats randomly placed over the reef substratum. Digital files were imported into Photoshop 7. An 11 × 11 unit uniform grid was superimposed over the image, and the shape of the original image was adjusted using the free transform function until the quadrat matched the grid. The coverage of massive *Porites* and *H. macrophysa* and other macroalgae was estimated by recording their presence under each of the 100 points where gridlines intersected. The abundance of contact boundaries between *Porites* and *H. macrophysa* was determined over four randomly placed belt transects (2 m width). The length of the *Porites-Halimeda* border was measured to the nearest centimeter on the first 4 to 6 colonies encountered per transect, totaling 20 colonies.

The macroalgal-removal experiment was performed in 2008. Thirteen colonies of massive *Porites* (diameter between 0.5 and 1.5 m) overgrown by *H. macrophysa* ($\geq$ 20 cm^2 of overgrown coral tissue surface area) were randomly selected within an area of ~500 m^2. Selected colonies were $\geq$ 2 m apart. Thalli of *H. macrophysa* and other canopy-forming macroalgal species were manually removed from all colonies by carefully lifting them up away from the coral surface. *Halimeda* and other macroalgae did not anchor on live coral tissue, so the removal process did not cause further damage to the underlying coral tissue. Selected colonies could have more than one patch of overgrowing *Halimeda*. However, all macroalgae were removed and only the largest patch of each colony was monitored and sampled. Our rationale was to follow the recovery of large overgrown patches with bleached coral tissue underneath (i.e., small patches had hardly any bleached tissue). The surface area of the exposed coral surface underneath large *H. macrophysa* patches ranged between 21 and 64 cm^2, which was <5% of the total colony surface area. The surface area that was cleared off in addition to the largest patch was negligeable and thus not recorded. We cannot exclude that the removed macroalgal canopy contained species other than *H. macrophysa*. However, these were inconspicuous and likely to have had negligeable impact.

Temporal changes in microbial communities were studied from two randomly chosen colonies, sampled immediately after macroalgal removal (day 0), and again on days 10, 25 and 40 avoiding re-sampling of colonies sampled previously. An air pressure-driven drill device was used to take 1 cm^2 cores of the coral tissue to a depth of approximately 1 cm. Two sample types were collected from each coral colony: (1) macroalgal-removed (or T = treated) samples in the previously overgrown area and (2) adjacent apparently healthy (or C = control) samples ~20 cm away from the previously overgrown part along the colony border (Fig. 2). Each sample consisted of three cores (total of 3 cm^2 of coral tissue surface area) drilled next (~1 cm) to each other and placed together in a separate container. The drill-bit was thoroughly cleaned underwater to reduce cross-contamination with sampled coral tissue between coring. Samples were brought to the surface and immediately

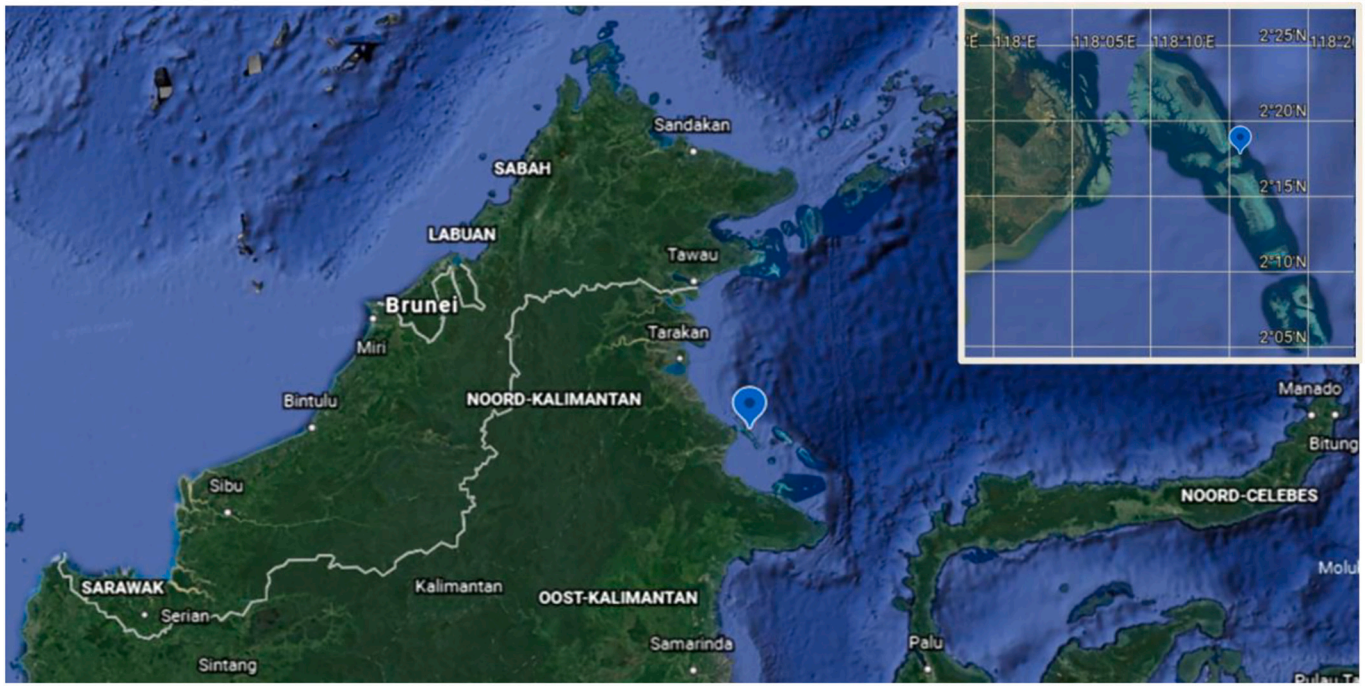

Fig. 1. Map of *E*-Kalimantan (Indonesia) showing the approximate location of Derawan island. In the inset the position of the small island of Derawan and the study site, Coral Garden, are indicated by the same pointer. Google Data SIO, NOAA, U.S. Navy, NGA, GEBCO Landsat/Copernicus.

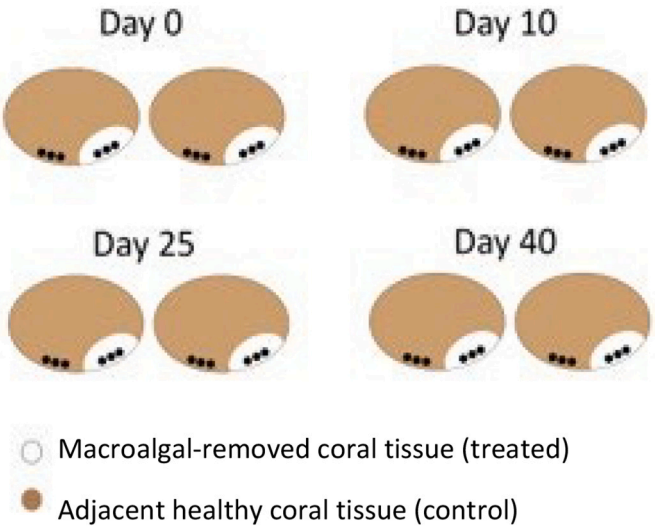

Fig. 2. Sampling scheme of the eight coral colonies. At each timepoint (Day) two coral colonies (replicates) were sampled by taking three 1 cm^2 coral tissue surface area cores in the control/healthy and three in the bleached part of the coral after removal of *H. macrophysa*. For each coral, the control/healthy coral tissue samples were joined. The same was done for the macroalgal-removed coral tissue samples.

submerged in RNAlater® (Life Technologies) to preserve nucleic acids during transport to the laboratory, where samples were kept frozen at −80 °C until further analysis.

To follow coral tissue recovery after removal of the macroalga on day 0, the bleached previously overgrown areas of, in total, 13 coral colonies were photographed. Eight of the 13 corals were only photographed at time points leading up to the time point of microbial sampling. Thus, 13 corals were photographed on day 0, 11 on day 10, 9 on day 25 and 7 on day 40. The areas of 'healthy' (normally pigmented, live coral tissue), 'bleached' (bleached live coral tissue with no dead tissue and no algal colonization) and 'severely bleached' (coral tissue/skeleton areas partially overgrown by a thin algal turf) coral under the initially overgrown areas were delineated and measured in Adobe Photoshop CS6. Adjacent apparently healthy areas (ca. 20 cm away from the overgrown areas) were used as control/healthy tissue. They were also photographed and visualized but, did not show any mortality or change in tissue coloration during the experiment. Colonies were not identified at the species level but, shared the same colony shape and polyp morphology as confirmed by observation using a magnifying glass. A temperature logger (Onset HOBO Pendant® Data Logger) recording data every 30 mins at the study site for 26 days during the experiment yielded a mean seawater temperature of 29.35 ± 0.61 (SD) °C (range: 25.0–30.5).

2.2. DNA extraction

A DNA extraction protocol for seawater samples (Wuchter et al., 2004) was used, which we adapted for the coral tissue DNA extraction. In brief, coral samples were transferred to 50 ml sterile Corning tubes with 10 ml extraction buffer (10 mM Tris HCL pH 8, 25 mM EDTA pH 8, 1 vol% SDS, and 100 mM NaCl). The coral samples were pulverized while submerged in the extraction buffer using a sterile spatula. The resulting tissue slurry underwent three freeze-thaw cycles using liquid nitrogen and subsequent heating to 40 °C. After each thaw step the slurry was homogenized for 10 min at maximum speed using a Vortex Genie homogenizer with 50 ml tube adapters (MO-BIO Laboratories Inc., Carlsbad, CA). The homogenized tissue slurry was extracted with 0.5 volumes of phenol pH 8, phenol/chloroform/isoamyl-alcohol (25:24:1), and chloroform. The DNA in the aqueous supernatant was then concentrated using 30KDa Amicon™ Ultra-4 centrifugal filter units (Millipore, Bedford, MA). DNA concentration was measured fluorometrically using Quant-iT™ PicoGreen® dsDNA reagent (Life Technologies, Carlsbad, CA). The quality of the DNA was verified through gel electrophoresis (30 min at 100 V, 2 wt% agarose gel).

2.3. Sequencing of 16S rRNA gene amplicons

The V4 region of the 16S rRNA gene was amplified with universal prokaryotic primers 517f (5′-GCC AGC AGC CGC GGT AA-3′) and 806r (5′-GGA CTA CCA GGG TAT CTA AT-3′) after Wuchter et al. (2013). The theoretical coverage of the primer combination was 91.0% of bacterial sequences and 92.3% of archaeal sequences available in the SILVA RefNR database ssu-138.1 according to a primer coverage test using TestPrime 1.0 allowing a maximum of two mismatches per primer while keeping a zone of 4 bases with 0-mismatch at the 3′ end (Klindworth et al., 2013). The formation of newly formed amplicons was followed in real-time using a Realplex quantitative PCR system (Eppendorf, Hauppauge, NY) (Coolen et al., 2009). The annealing temperature was set to 61 °C and reactions were stopped in the exponential phase after 25–30 cycles. To minimize the formation of artifacts such as primer dimers, 10^8 copies were subject to a second amplification reaction with the same region-specific primers that included the 454 fusion primer sequences (Wuchter et al., 2013). Each forward primer also included a unique ten base pair-long 454 Molecular Identifier (MID) barcode sequence to support the pooling of samples. The second qPCR run was stopped after only 12 cycles when all samples reached the end of the exponential phase. The quality of the PCR products was verified by agarose gel electrophoresis, and equimolar amounts of the barcoded PCR products were pooled and purified using the AMPure® XP PCR purification kit (Agencourt Bioscience Corp., Beverly, MA). Three micrograms of the pooled and purified barcoded amplicons were subjected to subsequent Roche 454 pyrosequencing using the facilities of Selah Genomics (Greenville, SC). The total number of sequences obtained was 70,260. The sequencing data are accessible via European Nucleotide Archive (ENA) under accession number PRJEB48224.

2.4. Filtering of reads and taxonomic assignment

Sequences were filtered by length (>250 bp) and their average Q score (>25) and sorted according to their MID identifiers using the Ribosomal Database project (RDP) pipeline initial process (Cole et al., 2014). A maximum of two mismatches was accepted in forward primer plus MID tags and the MID and forward primer sequences were removed in this step. Then, using the FastX toolkit in Galaxy (http://usegalaxy.org), sequences were trimmed from base 235 till the end, removing the reverse primer sequence and the regions with an average Q score < 35. The reads were classified using the SILVAngs web interface (Yilmaz et al., 2014) with default settings (OTU clustering at ≥98% and ≥ 93% classification similarity to the closest relative in the SILVA 132 database). Singletons were removed from the entire dataset.

2.5. Statistics and data exploration

Differences in the microbial OTU composition were visualized with nMDS plots based on Bray-Curtis similarity coefficients in PRIMER v7 (Clarke and Gorley, 2015). To compensate for differences in library sizes, the OTU counts were divided by the total number of reads in the respective sample. Further a square root transformation was applied to samples to dampen the effect of dominant OTUs and put more weight on less dominant OTUs. To compare the microbiome of macroalgal-removed versus adjacent control/healthy (control) coral tissue, and the influence of time (sampling days) on five taxonomic levels and the five most abundant classes, PERMDISP and PERMANOVA tests were performed (Anderson et al., 2015). Dispersions of macroalgal-removed and control/healthy group data were not significantly different at any taxonomic level (PERMDISP, $P > 0.05$). A mixed PERMANOVA model was used with treatment (macroalgal-removed vs control/healthy) and time (sampling days) as fixed factors, and coral colony as a random factor nested within time (Cti). Due to the limited number of degrees of freedom the interaction of time x treatment (not significant) and Cti x treatment (not significant) were left out of the model. To ensure complete independence in the interpretation of the significance of the factors, a Type III sum of squares partitioning was applied. For the nMDS plot and PERMANOVA tests all OTUs (excluding singletons and chloroplasts across all samples) were used.

We performed SIMPER analysis and indicator species analysis to investigate which OTUs characterized macroalgal-removed and adjacent control/healthy tissue and which OTUs were driving the dissimilarity between treatments. SIMPER analysis was used to identify the most influential OTUs (Clarke, 1993). SIMPER ranks variables (OTUs) based on their contribution to a sample group or based on their contribution to differences between groups (e.g., macroalgal-removed group vs adjacent control/healthy coral tissue group). OTUs that contributed up to 72.5% of the cumulative differences within and across sample groups were chosen. Indicator Species Analysis (ISA) was applied to identify OTUs with significant, nonrandom association ($P < 0.05$) to control/healthy vs macroalgal-removed coral tissue using the IndicSpecies package 1.6.7 in R (https://cran.r-project.org,version R-3.6.0, R Core Team) (De Cáceres and Legendre, 2009; Dufrêne and Legendre, 1997). Component 'A' is the estimate of the probability that the surveyed species (here: OTU) belongs to a group (control/healthy or macroalgal-removed group) given the fact that the species has been found. Component 'B' is the estimate of the probability of finding the species in a certain target group. SIMPER and IndicSpecies analysis tests were restricted to OTUs with >100 reads.

A persistent microbiome was defined to identify OTUs which are ubiquitous in control/healthy and macroalgal-removed coral tissue. This microbiome encompassed OTUs with assigned names of family, genus or group (≥93% cut-off) present (with one or more reads) in at least seven control/healthy and seven macroalgal-removed tissue samples of the eight coral colonies.

OTU alpha diversity was calculated using Shannon and Chao1 indices and compared in control/healthy vs macroalgal-removed coral tissue using a paired Student's *t*-test. The Shannon index combines species richness and their distribution (evenness) in one value, with the most weight on species richness. Chao1 is an abundance-based estimator of species richness and calculates expected OTUs based on observed OTUs.

Causal effect analysis was applied to identify microorganisms (OTUs) whose change in relative abundance would substantially influence the abundance of other microorganisms in the community. From the total number of OTUs (15,367), we selected OTUs with a sum of >50 reads across all samples to remove OTUs with a low number of reads, which might lead to spurious results in correlation-based network analyses. This filtering resulted in 152 OTUs. We added a pseudo-count of 1 to all OTUs in the filtered OTU table to allow applying variance stabilizing transformation (VST) (Anders and Huber, 2010). After VST, we selected OTUs with a base mean larger than one across samples, resulting in 47 OTUs. Next, we excluded sequences assigned to cyanobacterial chloroplasts. The remaining OTUs were subjected to causal effect analysis following a statistical algorithm called accumulation Intervention calculus when the Directed acyclic graph is Absent (aIDA) (Taruttis et al., 2015). We performed 100 subsamples with 80% of the samples included, and centered and scaled the features (OTUs) within each subsample before reconstructing the network with the PC algorithm, setting alpha to 0.2. We applied aIDA to estimate the causal effects of influential OTUs (>100 reads) which were selected from the indicator species and/or the SIMPER analyses, on all other OTUs (> 50 reads and base mean > 1 after VST) included in the network analysis.

To assess temporal variations, we included bacterial classes with a mean relative abundance above 5% (>3800 reads in 16 samples) and orders within these classes with a mean relative abundance of >2% (>500 reads in 16 samples). The difference in relative abundance of these classes and orders between the macroalgal-removed and adjacent control/healthy samples was determined. Differences in the relative abundance per class and order were used as relative to the control/healthy at each specific time point (i.e., macroalgal-removed at day

0 relative to control/healthy samples at day 0; macroalgal-removed at day 10 relative to control/healthy samples at day 10 etc.) and determined for each coral. Values were then averaged across the two colonies sampled at the same time point. Average differences of <1.5% (i.e., range of −1.5% to +1.5%) between macroalgal-removed and control/healthy samples were arbitrarily but conservatively considered as equal to the control/healthy samples. This % was based on measured differences ranging between −7% and + 7% in the average relative abundance of main classes and orders between control/healthy and macroalgal-removed samples at day 0 (just after algal removal). Certain trends in time of main classes and orders (when differences were > 1.5% between macroalgal-removed and control/healthy samples) were described.

3. Results

3.1. Coral-algal interactions and recovery of coral pigmentation

Massive *Porites* and *H. macrophysa* covered 7.6 ± 1.6 (SE) % and 2.4 ± 0.4%, respectively, of the reef bottom. Other macroalgae covered 1.0 ± 0.2%. Out of the 20 *Porites* colonies surveyed, 16 were partly overgrown by *H. macrophysa*, which was frequently found emerging from the dead coral crevices. We found that *Porites* colonies had a mean colony perimeter of 139.9 ± 20.1 cm, of which 15.2 ± 3.5 (10.8%) and 6.8 ± 1.6 (4.8%) cm contacted *H. macrophysa* and 'other macroalgae', respectively. *H. macrophysa* was always the dominant macroalga bordering *Porites* colonies.

A large percentage (71%) of coral tissue was bleached underneath *H. macrophysa* right after macroalgal removal (day 0) (Fig. 3, Table S1). The bleached tissue rapidly regained colour between day 10 and 25. An image of the three tissue classifications in Fig. 3 is presented in Fig. S1. On day 40, 90% of the previously bleached tissue had regained its full pigmentation.

3.2. Microbial diversity

In this study, 15,367 OTUs were assigned across all samples, with 6219 OTUs remaining after removing singletons. On average 3854 (SD 1632) high-quality reads were recovered per sample (range 1566–7003). Using a 98% sequence similarity cut-off, the average number of observed OTUs was 953 (SD 333) for macroalgal-removed coral tissue and 638 (SD 139) for adjacent control/healthy coral tissue.

The total OTU diversity (Shannon and Chao1 diversity indices) over the 40-day experimental period was significantly higher in macroalgal-removed than in adjacent control/healthy coral tissue (paired Student's

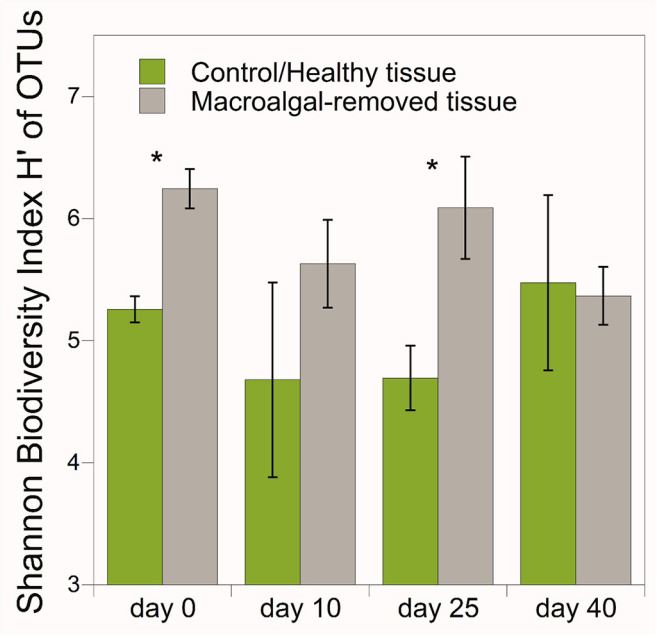

Fig. 4. Variations in the diversity index of the coral microbiome across treatments over time. Temporal variations in Shannon biodiversity index (bars indicate mean, error bars the range) of bacterial OTUs of control/healthy and macroalgal-removed tissue of *Porites* sp. * significant diversity difference between microbiome in control/healthy and macroalgal-removed tissue (paired *t*-test, $P < 0.05$).

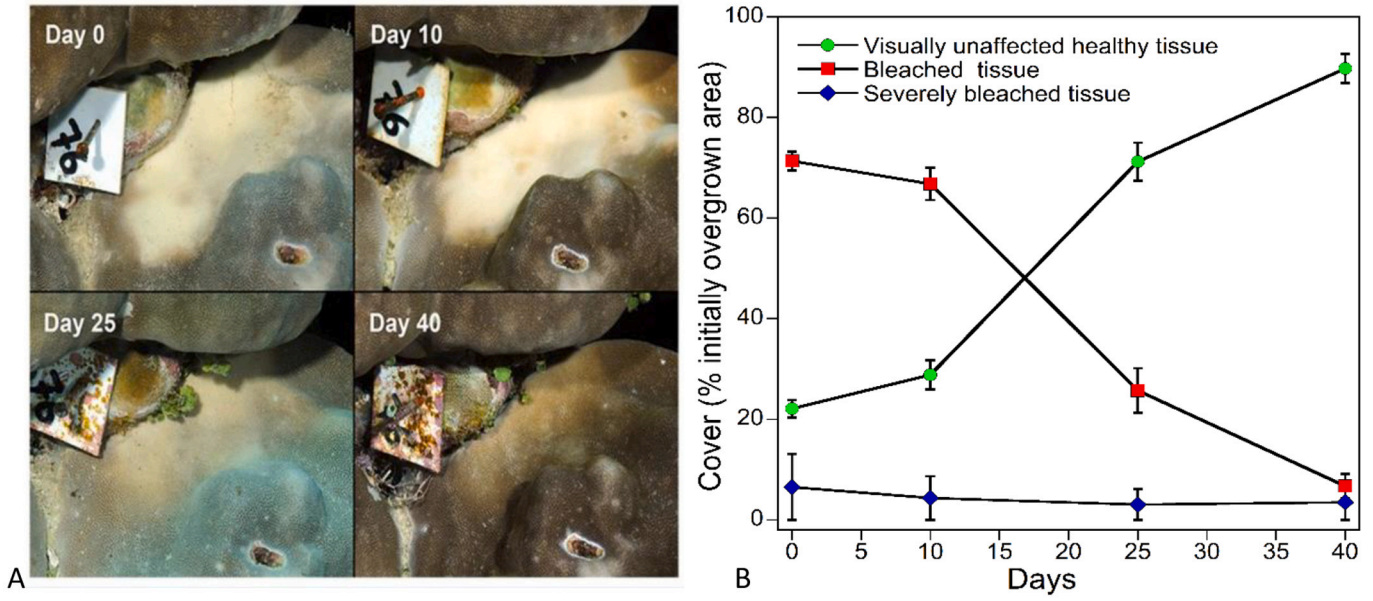

Fig. 3. Recovery of pigmentation in *Porites* after macroalgal removal. Monitoring of massive *Porites* surface area initially overgrown by *Halimeda macrophysa*. (A) Images show the return of symbiotic zooxanthellae (pigmentation) in the bleached part of the coral after removal of *H. macrophysa*. (B) Temporal changes in the cover percentage (mean ± SE, n = 7–13 colonies) of healthy, bleached and severely bleached coral tissue underneath the coral surface area initially overgrown by *H. macrophysa*.

t-tests, two tail: H′, $t = -2.776$, $P < 0.05$, Chao1, $t = -4.769$, $P < 0.01$, Fig. 4). On days 0 and 25 the diversity index differed significantly between the microbiome of control/healthy and macroalgal-removed tissue (paired Student's t-test, one tail; $P < 0.5$). Chao1 indicated that the sequencing effort was not enough to cover all distinct OTUs potentially present in the samples. According to this analysis, on average, 21,791 and 13,198 OTUs are expected in macroalgal-removed and adjacent control/healthy tissue of *Porites*, respectively. The rarefaction plot in Fig. S2 shows the differences in species richness of the 16 samples.

3.3. Microbiome composition

Most reads were mapped to the bacterial domain. Of these reads, 97% (SD 3%) were assigned to bacterial classes, and approximately 60% (SD 18%) to a bacterial genus (Table S2). A proportion of the reads assigned in SILVA 132 to the Oxyphotobacteria was falsely assigned to the alga *Ostreobium* (0.17% of reads) and unidentified chloroplasts (0.29% of reads). In addition, we found CAB-1, presumably a non-cyanobacterial phototrophic bacterium (Klaus et al., 2007). Control/healthy tissue (8 samples) contained 59 bacterial classes harboring 162 orders, whereas macroalgal-removed tissue (8 samples) contained 79 bacterial classes (including one unassigned class) with 198 orders over the 40-day experimental period.

Although the composition of the bacterial community was heterogeneous in the different coral colonies, coral samples (control/healthy and macroalgal-removed tissue), and on the different sampling days (Fig. 5), relative abundances of OTUs differed significantly between macroalgal-removed and adjacent control/healthy coral tissue, at class, order, family, genus and species level (Table 1A). There was no significant effect of time on the different taxonomic levels. The significance of the factor Coral(time) indicates that the eight corals sampled differed in microbial communities at the order and family level. PERMANOVA results of the main classes separately (with >3800 reads across all 16 samples) showed that macroalgal removal significantly ($P \leq 0.05$) affected the relative abundances of OTUs assigned to Gammaproteobacteria (1464 OTUs) and weakly affected OTUs assigned to Deltaproteobacteria (494), Alphaproteobacteria (1602) and Acidimicrobiia (347) respectively. OTUs assigned to Bacteroidia (801) were unaffected (Table 1B). Significant differences in time were found for the relative abundance of OTUs assigned to Alphaproteobacteria and Acidimicrobiia (Table 1B). Fig. 5 shows that on average the proportion of Gammaproteobacteria was higher in control/healthy than in macroalgal-removed tissue and that the proportion of Alphaproteobacteria, Deltaproteobacteria and Acidimicrobiia (Phylum Actinobacteria) was higher in macroalgal-removed than in control/healthy tissue.

3.4. Influential/indicator species and persistent members of the bacterial microbiome

The most influential OTUs in macroalgal-removed tissue (SIMPER) were assigned to *Mesorhizobium*, Rhizobiaceae (both Rhizobiales), Magnetospiraceae (Rhodospirillales) and Actinomarinales, and in control/healthy tissue Candidatus *Amoebophilus* GOS7BIJ07H004E (Cytophagales), *Janthinobacterium* (Betaproteobacteriales, Bulkholderiaceae) and *Asinibacterium* (Chitinophagales). Several OTUs were well represented in both control/healthy and macroalgal-removed coral tissue. The dissimilarity in microbiomes between macroalgal-removed and control/healthy tissue was 76% (SIMPER) with major contributions (>4%) by OTUs of *Janthinobacterium*, *Endozoicomonas* (Oceanospirillales) and Ca. *Amoebophilus* (Table 2, Table S3).

Significant indicator OTUs in macroalgal-removed coral tissue ($P \leq 0.05$, IndicSpecies test) were assigned to *Pseudovibrio*, an uncultured bacterium of Rhizobiaceaea (both Rhizobiales) and *Ruegeria* (Rhodobacterales). The control/healthy tissue harbored more significant indicator OTUs, notably *Janthinobacterium, Asinibacterium* (Chitinophagales), *Burkholderia-Caballeronia-Paraburkholderia* and *Ralstonia* (Burkholderiaceae), Ca. *Amoebophilus GOS7BIJ07H00WJ*, and two OTUs assigned to *Stenotrophomonas* (Xanthomonadales) (Table 2, Table S4).

The persistent microbiome, comprising genera present in at least 14 of the 16 samples, consisted of 28 out of 596 genera. Each member had >245 summed reads. The persistent microbiome harbored 16 (57%) genera (Table S5), which were also identified as influential and indicator genera based on SIMPER and Indicator-Species tests (Table 2).

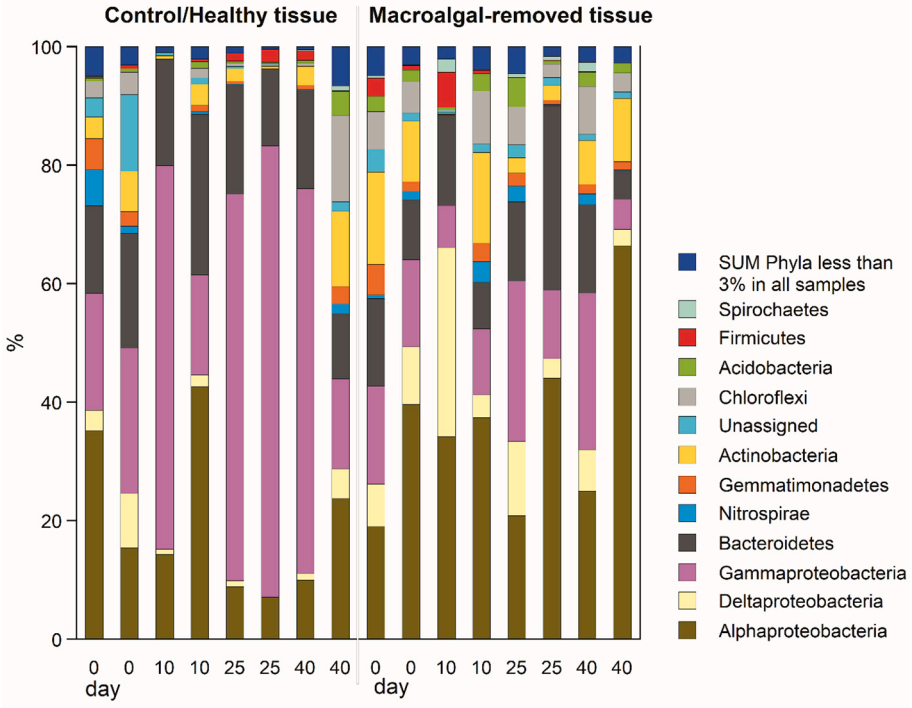

Fig. 5. Relative abundance of the dominant bacterial phyla/classes in *Porites*. Normalized distribution in phyla/classes in control/healthy and macroalgal-removed coral tissue in all eight corals sampled over time (SILVA132 classification). Note that the 1st bar in control/healthy and the 1st bar in macroalgal-removed tissue belong to one coral. The 2nd bar in control/healthy and alga-removed tissue belong to another coral (replicate coral at day 0). The same applies to bars at day 10, 20 and 40. It should be noted here that recently a reclassification of Deltaproteobacteria was proposed, splitting this functionally diverse class in four phyla (Waite et al., 2020).

Table 1
Multivariate analysis of microbiomes in macroalgal-removed and adjacent control/healthy coral tissue. PERMANOVA test results for OTUs assigned (A) to different taxonomic levels (68 classes, 180 orders, 319 families, 596 genera, 723 species, 5995 OTUs) and OTUs assigned (B) to main classes in the microbiome (with >3800 reads in 16 samples). Coral colonies were treated as random factor nested in time. Bold text shows at what taxonomic levels the microbial community composition differed significantly between categories. ($P \leq 0.05$), whereas P values >0.05 and ≤ 0.10 (italics) indicate weak to no significant differences in microbial communities between sample categories. OTU clustering and taxonomic assignments at class to species level were based on the 16rRNA SILVA SSU 132 data base.

A		Unique permutations	Class	Order	Family	Genus	Species	OTUs
Source	df		P	P	P	P	P	P
Treatment	1	9820	**0,01**	**0,02**	**0,02**	**0,02**	**0,03**	**0,04**
Time	3	105	0,43	0,49	0,53	0,35	0,33	0,17
Coral(time)	4	9936	*0,07*	**0,05**	**0,05**	*0,07*	*0,07*	0,12
Residual	7							
Total	15							

B		Unique permuta-tions	Gammaproteo-bacteria	Bacterioidia	Alphaproteo-bacteria	Deltaproteo-bacteria	Acidimicrobiia
Source	df		P	P	P	P	P
Treatment	1	9820	**0,02**	0,44	*0,10*	*0,06*	*0,08*
Time	3	105	0,87	0,60	**0,03**	0,89	**0,02**
Coral(time)	4	9936	*0,08*	0,20	0,51	**0,03**	0,17
Residual	7						
Total	15						

3.5. Shifts in the bacterial microbiome from control to treatment

The direction of change in the microbiome from control/healthy to macroalgal-removed tissue was comparable for all eight coral colonies despite large variations in microbial communities between colonies and different sampling times (Fig. 6). The consistent shift was mainly determined by a decrease in relative abundances of OTUs assigned to Gammaproteobacteria (i.e., *Janthinobacterium, Endozoicomonas, Stenotrophomonas* and Bacteroidia) and Ca. *Amoebophilus* GOS7BIJ07H004E in macroalgal- removed vs control/healthy tissue (Fig. 7, Table 2). An uncultured bacterium of the Magnetospiraceae (GOS7BIJ07H061K; Alphaproteobacteria, Rhodospirillales*)* was the key opposite vector of most Gammaproteobacteria (Fig. 7). Variations in the bacterial community of the eight coral colonies, irrespective of treatment (thus present in macroalgal-removed as well as control/healthy tissue of the coral) were determined mainly by the relative abundance of *Endozoicomonas* GOSBIJ07H009O, *Mesorhizobium* GOSBIJ07H00NJ, Rhizobiaceae and Actinomarinales (Fig. 7, Table 2). Specific genera explaining variability exclusively within the macroalgal-removed tissue were uncultured Rhodobacteraceae and *Pseudovibrio*. For the adjacent control/healthy tissue, this was mainly Ca. *Amoebophilus*.

3.6. Predicted causal interactions among OTUs

Causal effect analysis indicated that the most influential species for control/healthy (C) and both control/healthy and macroalgal-removed samples (B) among Gammaproteobacteria and Bacteroidia (Cytophagales) with >100 reads had a positive effect on the relative abundance of other OTUs with >50 reads and a base mean larger than one after variance-stabilizing transformation assigned to these (sub)classes (Fig. 8). For instance, influential OTUs belonging to Chitinophagales, Pseudomonadales, Betaproteobacteriales, and Xanthomonadales appear to enhance the abundance of other OTUs in these respective orders. The causal effects attributed to *Asinibacterium* (Bacteroidia, Chitinophagales) slightly deviated from the effects of other typical control OTUs in that it stimulates the relative abundance of a *Magnetospiraceae* GOSBIJ07H061K but depresses a Rhodobacteraceae (*Ruegeria* GOS7-BIJ07H0CUD) and Oceanospirillales (*Endozoicomonas* GOSBIJ07H069M/H009O). At the same time these depressed taxa are positively effectuated by all other control/healthy OTUs. The only control/healthy OTU, which ended up between the influential treatment OTUs after clustering (Fig. 8), was *Magnetospiraceae* GOSBIJ07H00LZ. It is predicted to have positive effects on the abundance of a Ca. *Amoebophilus* GOSBIJ07H0B3D (Bacteroidia, Cytophagales), an OTU which was not clearly positively affected by other influential control OTUs, except by *Asinibacterium*. In contrast, two other OTUs of Ca. *Amoebophilus* (GOS7BIJ07H0X9F, GOSBIJ07H004E) are predicted to be positively affected by control/healthy OTUs (C). *Mesorhizobium* GOSBIJH00NJ (Rhizobiales), being an influential OTU for both control/healthy and macroalgal-removed tissue species (B) showed positive effects on the abundance of Ca. *Amoebophilus* GOSBIJ07H0B3D/H004E and *Burkholderia-Caballeronia-Paraburkholderia* GOSBIJ07HH0B0W (Alphaproteobacteria, Betaproteobacteriales). Inhibiting effects of control/healthy OTUs *Endozoicomonas* GOSBIJ070NXT, *Stenotrophomonas* and *Ralstonia* were mainly directed against *Ruegeria* (Rhodobacterales), certain *Mesorhizobium* OTUs and uncultured Rhodothermaceae (Rhodothermales).

Typical influential macroalgal-removed sample OTUs (T) were predicted to exert fewer positive effects on the abundance of other OTUs in the community than typical control/healthy sample OTUs. Positive effects caused by influential macroalgal-removed sample OTUs assigned to Alphaproteobacteria in Rhodospirillales, Rhizobiales and Rhodobacterales (*Ruegeria*), were mainly observed targeting other OTUs in these orders. Influential macroalgal-removed sample OTUs assigned to Acidimicrobiia, Bacteroidia, and another Rhodobacteraceae exerted positive effects on the abundance of *Mesorhizobium*, an uncultured Rhizobiaceae and *Gilvibacter* (Flavobacteriales). Predicted adverse effects of typical macroalgal-removed sample species were most pronounced by an OTU assigned to an unknown Alphaproteobacterium. This taxon is likely to lower the relative abundance of various Rhizobiales (e.g., *Mesorhizobium*), *Gilvibacter,* and an uncultured Rhodothermaceae. The main inhibitor of Gammaproteobacteria was *Ruegeria* GOSBIJ07H04JW, most notably *Endozoicomonas* and, to a lesser extent, *Serratia* and *Escherichia-Shigella* (Enterobacteriales). Ca. *Amoebophilus* GOSBIJ07H004E, an influential OTU of the control/healthy samples was also predicted to be depressed by this *Ruegeria*. *Ruegeria* GOSBIJ07H041F was predicted to reduce the abundance of Ca. *Amoebophilus* GOS7BIJ07H0X9F, *Asinibacterium, Pseudomonas* (Gammaproteobacteria, Pseudomonadales), and *Escherichia-Shigella*.

3.7. Temporal variations in the bacterial microbiome

There was no significant effect of time on changes in the overall microbiome in macroalgal-removed tissue during the 40-day period. Variations in the microbiome of the control/healthy tissue as well as macroalgal-removed tissue of separate corals regularly exceeded

Table 2

OTUs/assignments with more than 100 reads, SIMPER and IndicSpecies test output and, OTU selection used in causal effect analysis. Shown are taxa that contributed >2.9% to similarities of samples belonging to the control/healthy (C) and macroalga-removed tissue (T) and those that contributed >1.5% to dissimilarities observed between C and T. For complete results of the SIMPER test see Table S3. Indicator species test results are presented by P values <0.2. Significant Indicator species have *P* values ≤0.05 (see Table S4 for 'A', 'B' and stat values of the IndicSpecies test). Empty cells refer to negligible contributions (SIMPER) with *P* values ≥0.2 (IndicSpecies). Selected OTUs (predicted to be influential and used for the causal effect analysis in Fig. 8) are indicated by letters C (control/healthy tissue), T (macroalga-removed tissue) and B (for both control/healthy and macroalga-removed tissue).

OTU_name	Class	Order	Family	Genus, Species	total_reads	Simper_C (%)	Simper_T (%)	Simper dissimilarity C and T (%)	indic_spec_C (P-value)	indic_spec_T (P-value)	OTU selection used in causal effect analysis
GOS7BIJ07H004E	Bacteroidia	Cytophagales	Amoebophilaceae	Candidatus Amoebophilus_unk_Sp	1474	14.31		4.31			C
GOS7BIJ07H005M	Gammaproteobacteria	Betaproteobacteriales	Burkholderiaceae	Janthinobacterium_uncultured bact	2345	6.21		5.08	0.034		C
GOS7BIJ07H009O	Gammaproteobacteria	Oceanospirillales	Endozoicomonadaceae	Endozoicomonas_uncultured bact	2428	4.09	5.24	4.69			B
GOS7BIJ07H06ZL	Bacteroidia	Chitinophagales	Chitinophagaceae	Asinibacterium_uncultured bact	229	6.06		1.99	0.024		C
GOS7BIJ07H01XQ	Gammaproteobacteria	Xanthomonadales	Xanthomonadaceae	Stenotrophomonas_unk_Sp	121	4.62					C
GOS7BIJ07H015Y	Gammaproteobacteria	Xanthomonadales	Xanthomonadaceae	Stenotrophomonas rhizophila	1184	5.11		3.77	0.016		C
GOS7BIJ07H01WM	Acidimicrobiia	Actinomarinales	Actinomarinales_uncultured	Actinomarinales_uncultured_bact	437	4.15	5.47	2.17			B
GOS7BIJ07H045H	Alphaproteobacteria	Rhizobiales	Stappiaceae	Pseudovibrio_unk_Sp	435		2.92	2.41		0.038	
GOS7BIJ07H01N2	Alphaproteobacteria	Rhizobiales	Rhizobiaceae	Rhizobiaceae_uncultured_bact	331		6.62	1.93		0.006	T
GOS7BIJ07H00NJ	Alphaproteobacteria	Rhizobiales	Rhizobiaceae	Mesorhizobium_unk_Sp	283	4.60	7.90	1.62			B
GOS7BIJ07H01AG	Alphaproteobacteria	Rhizobiales	Rhizobiaceae	Rhizobiaceae_unk_Gen_unk_Sp	252	3.33	6.96	1.52			B
GOS7BIJ07H09PJ	Gammaproteobacteria	Betaproteobacteriales	Burkholderiaceae	Burkholderia-Caballeronia-Paraburkholderia_unk_Sp	214	4.85		1.83	0.046		C
GOS7BIJ07H0B0W	Gammaproteobacteria	Betaproteobacteriales	Burkholderiaceae	Burkholderia-Caballeronia-Paraburkholderia_unk_Sp	213	4.93	2.94				B
GOS7BIJ07H04X2	Gammaproteobacteria	Betaproteobacteriales	Burkholderiaceae	Ralstonia_unk_Sp	170	3.19		1.63	0.032		C
GOS7BIJ07H00F4	Gammaproteobacteria	Betaproteobacteriales	Burkholderiaceae	Burkholderia-Caballeronia-Paraburkholderia_unk_Sp	152	3.01	3.25				B
GOS7BIJ07H02JF	Gammaproteobacteria	Enterobacteriales	Enterobacteriaceae	Serratia_unk_Sp	138	4.06	3.34				B
GOS7BIJ07H041F	Alphaproteobacteria	Rhodobacterales	Rhodobacteraceae	Ruegeria_unk_Sp	128		4.69	1.52		0.053	T
GOS7BIJ07H04JW	Alphaproteobacteria	Rhodobacterales	Rhodobacteraceae	Ruegeria_unk_Sp	110		4.88	1.60		0.008	T
GOS7BIJ07H002M	Alphaproteobacteria	Rhodospirillales	Magnetospiraceae	Magnetospiraceae_uncultured_bact	945		6.58	3.53			T
GOS7BIJ07H00LZ	Alphaproteobacteria	Rhodospirillales	Magnetospiraceae	Magnetospiraceae_uncultured_bact	660			3.08	0.060		C
GOS7BIJ07H03KN	Gammaproteobacteria	Pseudomonadales	Pseudomonadaceae	Pseudomonas_unk_Sp	350			1.93	0.101		C
GOS7BIJ07H03OY	Alphaproteobacteria	Rhizobiales	Stappiaceae	Pseudovibrio_unk_Sp	309			2.41		0.183	
GOS7BIJ07H0A12	Gammaproteobacteria	Xanthomonadales	Xanthomonadaceae	Stenotrophomonas_unk_Sp	202			1.57	0.030		
GOS7BIJ07H08K0	Bacteroidia	Flavobacteriales	Flavobacteriaceae	Gilvibacter_uncultured bact	198			1.68		0.134	T
GOS7BIJ07H00QS	Gammaproteobacteria	Betaproteobacteriales	Burkholderiaceae	Janthinobacterium_uncultured bact	185				0.089		
GOS7BIJ07H00WJ	Bacteroidia	Cytophagales	Amoebophilaceae	Candidatus Amoebophilus_unk_Sp	174			1.76	0.047		
GOS7BIJ07H004U	Acidimicrobiia	Microtrichales	Microtrichaceae	Sva0996 marine group_uncultured bact	169					0.106	T
GOS7BIJ07H061K	Alphaproteobacteria	Rhodospirillales	Magnetospiraceae	Magnetospiraceae_uncultured_bact	163		3.29				T
GOS7BIJ07H07NG	Gammaproteobacteria	Betaproteobacteriales	Burkholderiaceae	Janthinobacterium_unk_Sp	150				0.194		
GOS7BIJ07H0NXT	Gammaproteobacteria	Oceanospirillales	Endozoicomonadaceae	Endozoicomonas_uncultured bact	130				0.190		C
GOS7BIJ07H06IT	Alphaproteobacteria	Alphaproteobacteria_unk	Alphaproteobacteria_unk_C	Alphaproteobacteria_unk_Or_unk_fam_unk_Gen_unk_Sp	128		3.00				T
GOS7BIJ07H0EMB	Bacteroidia	Cytophagales	Amoebophilaceae	Candidatus Amoebophilus_uncultured bact	112				0.194		
GOS7BIJ07H02AC	Bacteroidia	KI89A clade	KI89A clade_unk_fam	KI89A clade_unk_fam_unk_Gen_unk_Sp	111					0.188	
GOS7BIJ07H00BN	Gammaproteobacteria	Rhodobacterales	Rhodobacteraceae	Rhodobacteraceae_unk_Gen_unk_Sp	108		3.43				T
GOS7BIJ07H03UG	Rhodothermia	Rhodothemales	Rhodothermaceae	Rhodothermaceae_uncultured_bact	1258			1.67			
GOS7BIJ07H0346	Alphaproteobacteria	Rhizobiales	Beijerinckiaceae	Methylocella palustris	234			1.84			

variations between macroalgal-removed and coral/healthy tissue (Fig. 5). The only classes of which the relative abundances were significantly affected by time were Alphaproteobacteria and Acidimicrobiia (Table 1B). Furthermore, there were alternating temporal patterns in certain classes and orders in macroalgal-removed coral tissue relative to adjacent control/healthy tissue (Fig. 9). The average relative difference in main classes (>3800 reads in 16 samples of eight corals) between macroalgal-removed and adjacent control/healthy coral tissue on day 0 was small compared to the differences observed on days 10, 25 and 40 (Fig. 9A). Absolute average differences increased from day 0 to day 10 and/or 25 and slightly declined to day 40 for most classes. Specific orders of Gammaproteobacteria (Fig. 9B), Bacteroidia (Fig. 9C), and Desulfovibrionales (Fig. 9F) adhered to this trend of temporal changes. Noteworthy are average depletions in Oceanospirillales, Betaproteobacteriales (Fig. 9B) and Cytophagales (Fig. 9C) compared to the control/healthy samples. Alphaproteobacteria increased in time

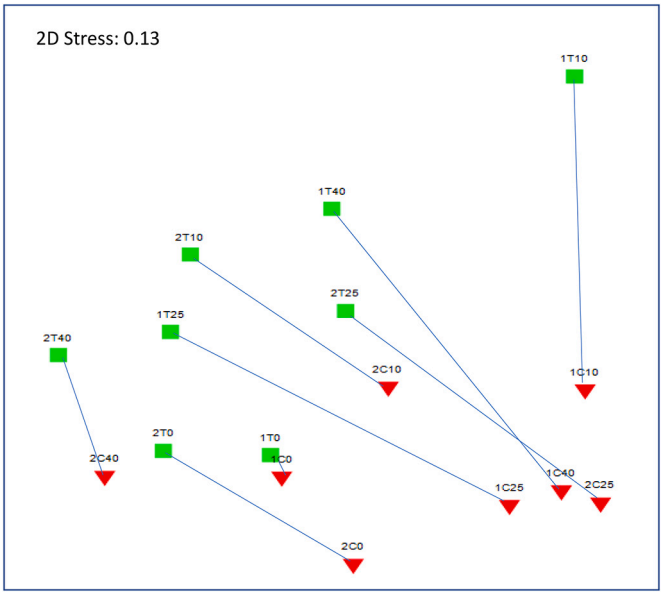

Fig. 6. Difference in the bacterial microbiome between treatments. Non-metric Multidimensional Scaling (nMDS) plot of the microbiome (OTUs) of algal-removed and adjacent healthy tissue of each *Porites* coral colony on day 0, 10, 25 and 40 after removal of the alga *Halimeda macrophysa*. Bray-Curtis dissimilarities were used. Lines connect adjacent control/healthy (red symbols and C letters) and macroalga-removed (green symbols and T letters) microbiomes of the same coral colony. Numbers 1 and 2 preceding C or T letters refer to replicate colonies sampled at day 0, 10, 25 and 40.

(Fig. 9A) mainly due to an increased abundance of Rhizobiales and Rhodobacterales relative to the control/healthy samples (Fig. 9D). Rhodospirillales and Rhodovibrionales showed a different trend with relative abundances increasing from day 0 to 25 and declining towards day 40. Main orders in Acidimicrobiia (Actinomarinales and Microtrichales) returned within 25 days (Fig. 9E) to the low relative abundance as found in the control/healthy samples (within −1.5 to +1.5% difference). Ten days after removal of the macroalgae, Desulfovibrionales (*Desulfovibrio*) had steeply increased in one of two samples (Fig. 9F). Orders NB1-j and Myxococcales (Deltaproteobacteria) reached the highest average differences (+2.9% each) with the control/healthy sample 25 days after the removal of macroalgae before returning to <1.5% difference with the control/healthy sample at day 40. It should be noted that the assignment Deltaproteobacteria in Fig. 9A was based on SILVA 132 classification. Deltaproteobacteria were recently placed into new separate phyla (Desulfobacterota phyl. Nov., Myxococcota phyl. Nov. and Bdellovibrionota phyl. Nov.) and classes (Waite et al., 2020). Orders mentioned in Fig. 9F (except NB1-j) would move in the reclassification under the corresponding new phyla. Therefore, this proposed reclassification would not affect the differences between the relative abundance of orders in control/healthy and macroalgal-removed tissue.

Of the 25 orders in Fig. 9B-F, 32% differed from the control/healthy samples at day 0, 36% at day 10, 52% at day 25 and 36% at day 40. Five of the 25 orders with >500 reads in 16 samples of eight corals did not exceed the 1.5% difference with the control during the 40-day experiment.

4. Discussion

Despite the relatively low numbers of reads (inherent to the methods used in 2009) and low number of replicates (two samples per treatment) our study showed that macroalgal contact and the amount of time past after removal of macroalgal overgrowth resulted in significant changes in the coral microbiome. As such, our study contributes to capturing the dynamics of the bacterial microbiome in stress recovery. Caution in the generalizability of these results is recommended, though. Our observed patterns in the coral microbiome over time will motivate future research in this field.

4.1. Macroalgal removal and recovery of pigmentation

Experimental removal of *Halimeda macrophysa* alleviated the exposed coral tissue instantaneously from contact stress. Compared to other seaweeds *Halimeda* excretes relatively low levels of DOM (Mueller et al., 2014; Nelson et al., 2013), and shows relatively low allelochemical activity, as suggested by the settlement of coral larvae on their segments (Nugues and Szmant, 2006). Therefore, it was not surprising

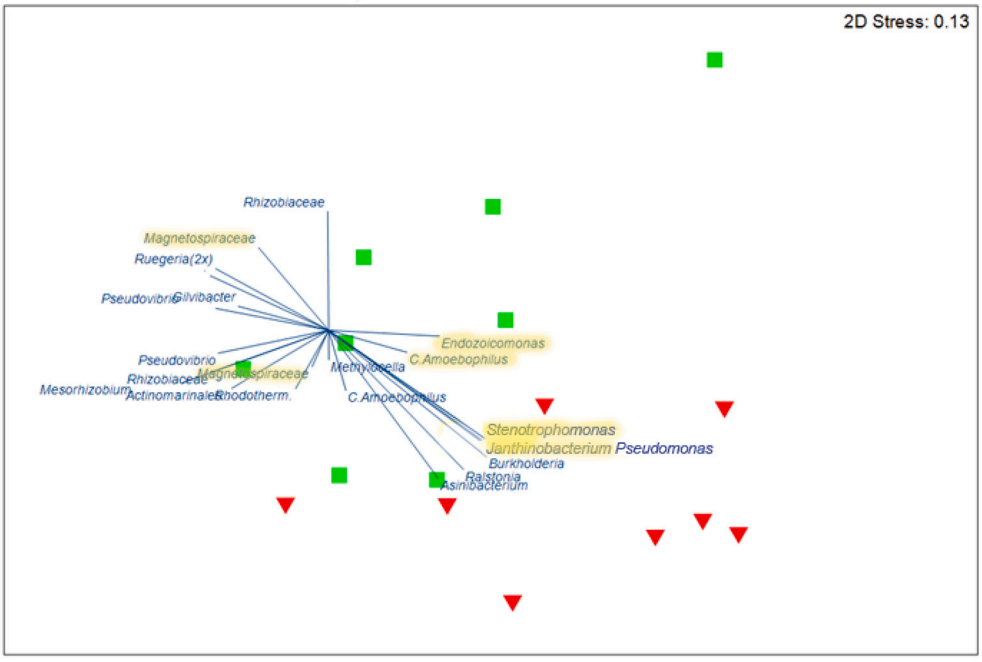

Fig. 7. Main bacterial taxa based on OTUs characterizing the dissimilarity between treatments. nMDS plot of Fig. 6. overlaid by a Principal Component Analysis (PCA) with vectors of OTUs (classified until genus level) with contributions of >1.5% (maximum 5.08%) to the dissimilarity between adjacent healthy coral tissue (red symbols) and algal-removed coral tissue (green symbols). The Genera/Families showing the strongest dissimilarities between control/healthy and macroalgal-removed microbiomes (>2.9%) are highlighted. *Ruegeria (2×)* refers to two distinct OTUs. Samples are detailed in Table 2.

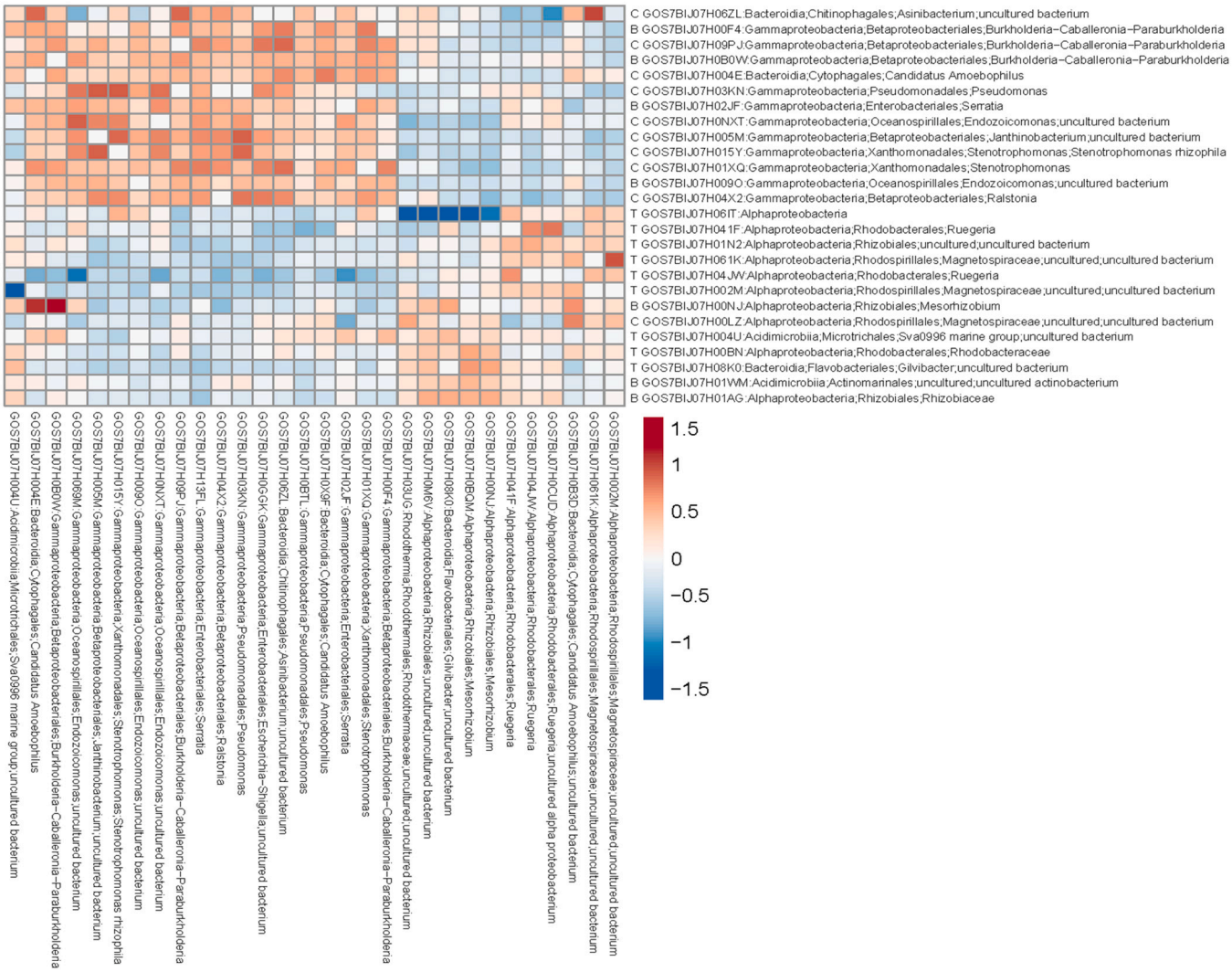

Fig. 8. Causal effect heatmap. Causal effects of influential OTUs of control/healthy coral tissue, macroalgal-removed coral tissue and both tissue types with relatively abundant species (OTUs) in the microbiome (influential species are listed in Table 2). Each individual cell of the heatmap displays the causal effect of an influential OTU (Y-axis) on another OTU (X-axis). Along the X-axis only the top 30 OTUs (with >50 reads in 16 samples) receiving the largest causal effects are shown. The Y-axis lists the causal OTUs affecting the OTUs on the X-axis. Names of influential OTUs (Y-axis) which are indicative of macroalgal-removed and apparently healthy coral tissue samples are preceded by a 'T' and 'C', respectively, and OTU names which are influential in both groups are preceded with a 'B'. Family names were omitted whenever a genus name was assigned to the OTU. The colour of the cells of the heatmap indicate causal effect size, that is, if the abundance of the causal OTU changes by one standard unit, how much the affected OTU will change in abundance (in standard units). Red colors indicate positive effects and blue colors negative effects.

that underneath the area overgrown by *Halimeda*, the coral tissue was predominantly bleached implying that it was still alive but had lost its zooxanthellae which is a well-known stress response in corals (Obura, 2009).

After the removal of *Halimeda* the exposed bleached tissue pigmentation largely returned between day 10 and 25 (Fig. 3). At day 40, coloration did not differ between macroalgal-removed vs adjacent control/healthy tissue. A comparable recovery of photosymbionts and photosynthesis after an unforeseen short-time disturbance leading to bleached corals in vitro was described for *Montastrea faveolata* (Rodríguez-Román et al., 2006). Coral overgrowth by algae represents chronic but localized stress, as opposed to colony-wide stress in the case of bleaching due to elevated seawater temperature. In this latter case, CO_2 fixation function is impaired, and recovery of photosymbionts takes much longer than 40 days (Jones et al., 1998). Only partial recovery in chlorophyll-a concentration and zooxanthellae densities in various coral species occur within 25 days (Hueerkamp et al., 2001), and complete recovery of zooxanthellae densities in partly bleached corals due to heat stress typically takes 3 to 7 months (Gleason, 1993; Jones and Yellowlees, 1997; Lang et al., 1992). Recovery of fully bleached corals may even require up to 2 years (Glynn and D'Croz, 1990). Rapid recovery of pigmentation in our study implies that *Halimeda macrophysa* contact induced a mild stress response of *Porites* sp.. The fact that an average of ca. 15% of coral colony perimeter interacted with macroalgae (ca. 10% with *H. macrophysa* and ca. 5% with other macroalgae) may also have contributed to the relatively mild effect of *H. macrophysa* on *Porites* sp. and the rapid recovery of the latter.

4.2. Major differences in the coral microbiome between treatments

Despite large inter-colony variation in the bacterial microbiome (Figs. 5, 6), a significant modification of the microbiome due to macroalgal contact was established in agreement with previous findings (Bourne et al., 2016; Brown et al., 2019; Morrow et al., 2013; Morrow et al., 2012; Roach et al., 2020; Smith et al., 2006; Vega Thurber et al., 2012). Interestingly, time passed since removal of the macroalga (up to

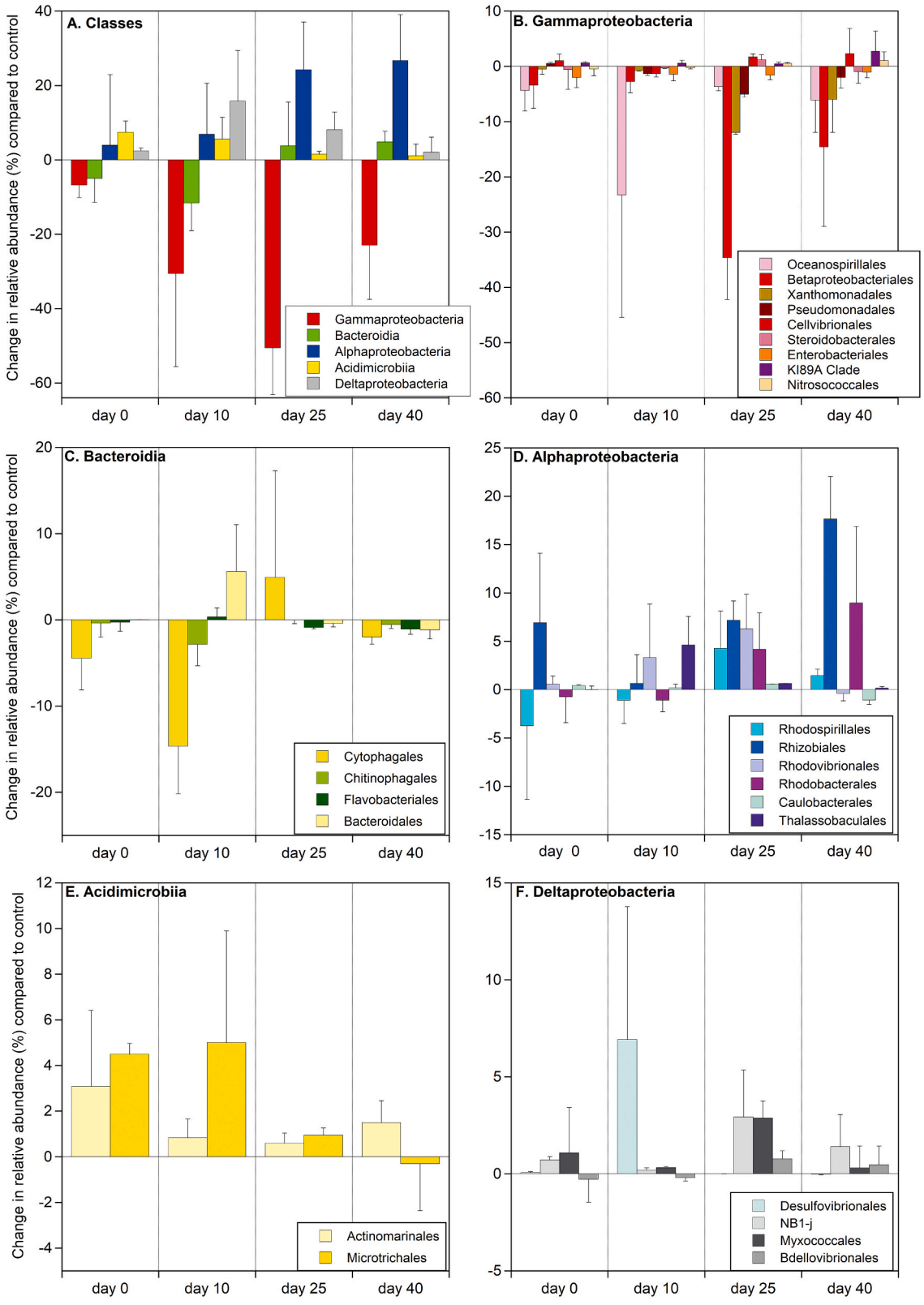

Fig. 9. Effect of macroalgal removal on main bacterial classes and orders over time. Mean deviation of relative abundance (error bars indicate half the range in %) in the macroalgal-removed compared to the adjacent control/healthy (0%) coral tissue as a function of days since algal removal for: (A) classes of Bacteria and (B) orders of Gammaproteobacteria, (C) Bacteroidia, (D) Alphaproteobacteria, (E) Acidimicrobiia and (F) Deltaproteobacteria. Classes with >3800 and orders with >500 reads in all samples (8 control/healthy, 8 macroalgal-removed samples) were used. Negative values indicate that the relative abundance in the macroalgal-removed tissue was lower than in the control/healthy tissue and positive values indicate that the relative abundance in the macroalgal-removed group was higher than in the control/healthy group. Considering the proposed reclassification of Deltaproteobacteria (Waite et al., 2020) the orders in (F) might be assigned to four different phyla.

40 days) had no significant effect on the microbiome in the macroalgal-removed tissue samples. This was unexpected considering the relief of contact stress (physical contact, light, chemistry) and return of pigmentation in the bleached tissue. The return of zooxanthellae is considered a driving force in the recovery of coral microbiomes after a bleaching event (Bourne et al., 2008). Growing algal symbionts may however retain photosynthates after bleaching, delaying the recovery of the coral host and its microbiome (Wooldridge, 2013).

Differences in the microbiome of macroalgal-removed and adjacent control/healthy coral tissue varied in magnitude between colonies and appeared to shift in a similar manner (Fig. 6). Algal overgrowth by *Halimeda* may induce an adaptation of the microbiome, which is comparable across colonies and persists several weeks after removal of the macroalgae. This parallel response is likely due to the resident/individual microbiome of *Porites*, which appears to be relatively stable and reacts similarly to the same disturbance (Ainsworth et al., 2015; Claar et al., 2020; Hernandez-Agreda et al., 2018). The overall effect of macroalgal overgrowth and subsequent relief of the disturbance on the microbiome appeared to be the suppression of Gammaproteobacteria and Bacteroidia and an increase in the relative abundance of Alphaproteobacteria and microbial diversity (mainly within Alphaproteobacteria). Enhanced microbial diversity in corals has been suggested to be indicative of a disruption in the natural balance of the microbiome and a ubiquitous sign of stress (McDevitt-Irwin et al., 2017; Vega Thurber et al., 2012; Zaneveld et al., 2016). The shift in the microbiome from Gammaproteobacteria to a higher relative abundance of Alphaproteobacteria initiated by macroalgal contact and contact removal does not necessarily contradict with results of others (Kelly et al., 2014), who compared the microbiome of "healthy" corals under different environmental conditions. Kelly et al. (2014) found that algae-dominated reefs favor a microbiome dominated by Gammaproteobacteria as opposed to Alphaproteobacteria in a coral-dominated reefs microbiome. However, the genus *Porites* appears to maintain a stable bacterial assemblage of Gammaproteobacteria regardless of environmental fluctuations (Dunphy et al., 2019; Johnston and Rohwer, 2007; Morrow et al., 2013; Pootakham et al., 2017; Sunagawa et al., 2010). In our study stress initiated by macroalgal contact affected the balance between different classes with higher relative abundances of Alphaproteobacteria and Acidimicrobiia than Gammaproteobacteria and Bacteroidia in macroalgal-removed compared to control/healthy samples. SIMPER dissimilarity in microbiomes between treatments was mainly caused by OTUs assigned to *Janthinobacterium*, *Endozoicomonas*, *Stenotrophomonas rhizophila* (all Gammaproteobacteria), while Ca. *Amoebophilus,* and Bacteroidia (Table 2) were clearly suppressed in the macroalgal-removed tissue. Not surprisingly, OTUs assigned to these taxa were relatively abundant in the control/healthy coral tissue of *Porites* and part of the persistent microbiome. These taxa also form part of the core microbiome in various other coral species (Ainsworth et al., 2015; Bayer et al., 2013; Hernandez-Agreda et al., 2018; Morrow et al., 2012; Neave et al., 2016) and may be beneficial for corals (Peixoto et al., 2017). In the Alphaproteobacteria, various OTUs assigned to the Rhodospirillales, Rhizobiales and Rhodobacterales and Acidimicrobiia dominated the balance in macroalgal-removed samples and were also present in adjacent control/healthy tissue contributing to the persistent microbiome although at lower relative abundances. Known pathogenic *Vibrio*'s (Vibrionales) in corals (Sweet et al., 2013) were not found in the macroalgal-removed coral tissue. Only *Serratia* (Enterobacteriales, Gammaproteobacteria), represented by the necrotizing coral pathogen *Serratia marescens* (Ritchie, 2006), might cause disease. The OTU assigned to *Serratia* in our study was present at low relative abundances (0.2 and 0.9%, respectively) in both macroalgal-removed and adjacent control/healthy tissue. Therefore, a substantial negative impact of *Serratia* on the health of *Porites* in our study was unlikely. The observation that the microbiome with 28 shared genera in control/healthy as well as macroalgal-removed tissue (albeit at different relative abundances) persisted during the 40-day period and that 57% of these genera were influential in control/healthy and macroalgal-removed tissue, may suggest that these species play a role in stabilizing the microbiome forming the core microbiome (sensu Hernandez-Agreda et al., 2018). Whether this group plays a role in the recovery or in resisting change in the microbiome remains unclear. Nevertheless, it is evident that within 40 days after removal of the macroalgal overgrowth, the microbial community, unlike pigmentation, did not return to the pre-disturbance community in the control/healthy tissue.

The causal effect analysis (Fig. 8) suggests recovery potential as shown by the overall positive influence of typical species in control/healthy tissue on the relative abundance of Gammaproteobacteria and Bacteroidia. In contrast, the influence of typical species of macroalgal-removed tissue (mainly Alphaproteobacteria) was not clear because positive as well as negative effects on the control/healthy microbiome were predicted. This suggests that most control/healthy OTUs benefit from each other. In contrast, some OTUs in macroalgal-removed tissue might support a return to the control state, while others are likely to inhibit this process. Antagonism can be a structuring force in coral-associated microbial composition (Rypien et al., 2009). Causal effect analysis is based on the observed variation in microbial abundances. Estimated effects converge to true effects with very large sample sizes and all network nodes (members) being observed. This scenario is unlikely for biological systems, especially involving protected species; therefore predicted effects need to be interpreted cautiously. However, they are a first step in understanding the driving forces in an interconnected system such as microbial communities, and a promising tool to generate hypotheses for experimental follow-up. The observed inter-colony heterogeneity may have complicated the assessment of significant shifts in the microbiome over time. Interactions among bacterial species likely contributed to heterogeneity in the microbiome of control/healthy and macroalgal-removed coral tissue with considerable differences in the microbiome between colonies of the same coral species. This may well be in accordance with observations that resident/individual microbiomes (sensu (Hernandez-Agreda et al., 2018) do not respond equally to environmental disturbances and vary with several factors, such as colony age and shedding of mucus layer (Glasl et al., 2016; Williams et al., 2015).

4.3. Temporal patterns in subgroups of the bacterial microbiome

Although the bacterial microbiome did not significantly change in time after removal of the macroalga, subgroups (Alphaproteobacteria and Acidimicrobiia) demonstrated temporal patterns relative to the control suggestive of consistent directional shifts during the 40-day period. The removal of macroalgae resulted in various deviations (increases as well as decreases) in average relative abundances in subgroups from the control/healthy samples over time. The sudden exposure of the macroalgal-removed tissue to increased light and change in nutritional conditions after the removal of *Halimeda* appeared to exacerbate the stress and initiated a biphasic temporal response of certain classes and orders.

In the first phase, from day 0 to 10, the relative increase in Rhodovibrionales (Alphaproteobacteria) and Desulfovibrionales (Deltaproteobacteria) could be an adaptation to change in light and oxic conditions in the still bleached coral tissue that favors anaerobic metabolisms such as sulfate reduction and nitrogen fixation (Diaz, 2017; McDevitt-Irwin et al., 2017; Rodríguez-Román et al., 2006). The average increase of Bacteroidales may indicate increased susceptibility to coral disease, while Thalassobaculales may herald an increase in zooxanthellae. Contemporaneously, the declines of Cytophagales (dominated by Ca. *Amoebophilus*), and Oceanospirillales (dominated by *Endozoicomonas*), which tend to be closely associated with their coral host (Ainsworth et al., 2015; Huggett and Apprill, 2019) may concur with a loss of antimicrobial and phagocytic activities (Mahmoud and Kalendar, 2016; Welsh et al., 2016). Abrupt environmental changes induced by the removal of the macroalga led within 10–25 days to the return (decrease)

of Actinomarinales and Microtrichales (Acidimicrobiia) to their relative abundances in control/healthy microbiome. This retreat concurred with an increase of Alphaproteobacteria, suggestive of repression of certain Microtrichales by Alphaproteobacteria (e.g., Rodospirillales, Magnetospiraceae, Fig. 9).

During the second phase from day 10 to 40 Rhizobiales and Rhodobacterales (Alphaproteobacteria) most notably increased in average relative abundances compared to the microbiome of control/healthy tissue. Rhodobacterales are opportunistic colonizers and have been found in relatively high abundance in stressed corals (Welsh et al., 2017; Zaneveld et al., 2016). Also, the co-occurrence of enhanced relative abundances of Rhodobacterales and Rhizobiales has been linked to diseased corals (Rosales et al., 2020). The declines in Betaproteobacteriales, Xanthomonadales and Pseudomonadales (Gammaproteobacteria) relative to the healthy tissue from day 10 to 25 and their subsequent increases by day 40 coincided with inverse patterns of Rhodospirillales and Rhodovibrionales (Alphaproteobacteria), which may indicate antagonistic interactions between species of Alpha- and Gammaproteobacteria over time. Based on established causal interactions and temporal patterns, it appears that *Ruegeria* (GOSBIJ07H04JW, Rhodobacterales) negatively influenced certain *Endozoicomonas, Serratia* (Gammaproteobacteria), and Bacteroidia from day 10 to 40. *Mesorhizobium* (Rhizobiales) may have played a role in the reestablishming two influential species of the adjacent control/healthy coral tissue (Ca. *Amoebophilus* GOS7BIJ07H004E and *Burkholderia-Caballeronia-Paraburkholderia* GOSBIJ07H0B0W). These examples support the notion that Alphaproteobacteria may play an essential role in structuring the microbiome after a disturbance in time. Their presence in the persistent microbiome possibly bears witness to this role under prevailing environmental conditions. In addition, the return of zooxanthellae and reestablishment of symbiotic relationships with zooxanthellae may have reversed the decline of Gammaproteobacteria towards an increase from day 25 onwards. However, although the average abundance did not return to that in adjacent control/healthy tissue. The recovery of Gammaproteobacteria might still be hampered by limited transfer of photosynthates of symbionts to the host and/or to low densities of zooxanthellae in the macroalgal-removed tissue on day 40, despite visual assessments showing a return to pigmentation (Bourne et al., 2013; Morrow et al., 2013).

One could argue that (1) the microbiome dominated by Alphaproteobacteria in the macroalgal-removed tissue forms a stable microbiome adjacent to one dominated by Gammaproteobacteria in the control/healthy tissue on the same colony after 40 days. The presence of distinct microbiomes on a single coral colony (Damjanovic et al., 2020) and between coral clones of a given genotype (Dubé et al., 2021) have been reported previously. This explanation is consistent with the large variations in the microbiome between individual corals in control/healthy as well as macroalgal-removed tissue (Fig. 5). Another option is that (2) recovery of the microbiome in the macroalgal-removed tissue was still ongoing after 40 days considering trajectories of change observed in subgroups. Forebodes of recovery might be the return of Rhodospirillales, Rhodovibrionales, Actinomarinales, and Microtrichales in macroalgal-removed samples to average abundances found in control/healthy tissue and the return of diversity in macroalga-removed samples to the diversity in the healthy tissue after 40 days. Whether the observed sequence in changes of certain orders during the experiment represents a predictable trajectory towards a stable microbiome is plausible but remains to be investigated.

5. Conclusions

This study shows that macroalgal overgrowth affects the coral microbiome and that, despite a quasi-complete recovery in coral tissue pigmentation, bacterial microbiome recovery after removal of the macroalga is not achieved in 40 days, however with indications that recovery was still ongoing. The overall effect of macroalgal overgrowth on the microbiome appeared to be the suppression of Gammaproteobacteria and Bacteroidia and an increase in microbial abundance of Alphaproteobacteria and diversity (mainly within Alphaproteobacteria). The positive influence of indicator and other influential species on the relative abundance of other coral microbiome members suggest recovery potential of the coral microbiome to macroalgal overgrowth. Observed alternating patterns in the relative abundance of subgroups in macroalgal-removed compared to control/healthy tissue over time indicates that subgroups in the microbiome are adapting to the changing environmental circumstances in a quasi-consistent way. However, the relatively high abundance of Rhizobiales and Rhodobacterales from day 25 onwards suggests that the coral colonies still experienced stress. Longer time series (>40 days) are required to assess whether full recovery of the coral microbiome after macroalgal removal is achievable.

Funding

This research was supported by the Netherlands Organization for Scientific Research (NWO-WOTRO).

Grant disclosure

NWO-WOTRO Science for Global Development grant WT 84–617.

Author contributions

Fleur C. van Duyl conceived the field experiments and was the main author.

Judith D.L. van Bleijswijk supervised the molecular analyses, authored drafts of the manuscript and approved the final draft.

Cornelia Wuchter performed the DNA extractions and created the 16S amplicon library.

Harry J. Witte carried out most statistical analyses.

Marco J.L. Coolen contributed to DNA analysis costs, reviewed drafts of the manuscript and approved the final draft.

Julia C. Engelmann performed the causal effect analyses and approved the final draft.

Rolf P.M. Bak reviewed and approved the final draft.

Maggy M. Nugues designed and conducted the field experiments, authored and reviewed drafts of the manuscript and approved the final draft.

Field study permission

Permission was granted by the Departemen Dalam Negeri (Domestic Department), Republik Indonesia. Direktorat Jenderal Kesatuan Bangsa dan Politik (General Director of National and Political Unity). Surat Pemberitahuan Penelitian (Research Notification Letter): Nomor (Nr) 070/1241.D.III.

Declaration of Competing Interest

The authors of the manuscript entitled “Recovery patterns of the coral microbiome after relief of algal contact” declare that they have no conflict of interest in relation to the research activities. The authors agreed to submit the manuscript to the Journal of Sea Research.

Data availability

Data will be made available on request. Sequences are accessible via European Nucleotide Archive (ENA) accession number PRJEB48224.

Acknowledgements

We thank Gerard Nieuwland for logistical support during the fieldwork in Indonesia and labwork at NIOZ, Texel, NL.

Appendix A. Supplementary data

Supplementary data to this article can be found online at https://doi.org/10.1016/j.seares.2022.102309.

References

Ainsworth, T.D., Krause, L., Bridge, T., Torda, G., Raina, J.-B., Zakrzewski, M., Gates, R. D., Padilla-Gamiño, J.L., Spalding, H.L., Smith, C., Woolsey, E.S., Bourne, D.G., Bongaerts, P., Hoegh-Guldberg, O., Leggat, W., 2015. The coral core microbiome identifies rare bacterial taxa as ubiquitous endosymbionts. ISME J. 9, 2261–2274. https://doi.org/10.1038/ismej.2015.39.

Anders, S., Huber, W., 2010. Differential expression analysis for sequence count data. Genome Biol. 11, 106. https://doi.org/10.1186/gb-2010-11-10-r106.

Anderson, M.J., Gorley, R.N., Clarke, K.R., 2015. PERMANOVA+ for PRIMER: Guide to Software and Statistical Methods. PRIMER-E, Plymouth, Unite Kingdom.

Barott, K.L., Rohwer, F., 2012. Unseen players shape benthic competition on coral reefs. Trends Microbiol. 914, 8.

Barott, K.L., Rodriguez-Brito, B., Janouskovec, J., Marhaver, K.L., Smith, J.E., Keeling, P., Rohwer, F.L., 2011. Microbial diversity associated with four functional groups of benthic reef algae and reef-building coral *Montastraea annularis*. Environ. Microbiol. 13, 1192–1204. https://doi.org/10.1111/j.1462–2920.2010.02419.x.

Barott, K.L., Rodriguez-Mueller, B., Youle, M., Marhaver, K.L., Vermeij, M.J.A., Smith, J. E., Rohwer, F.L., 2012. Microbial to reef scale interactions between the reef-building coral *Montastraea annularis* and benthic algae. Proc. R. Soc. B 279, 1655–1664.

Bayer, T., Neave, M.J., Alsheikh-Hussain, A., Aranda, M., Yum, L.K., Mincer, T., Hughen, K., Apprill, A., Voolstra, C.R., 2013. The microbiome of the Red Sea coral Stylophora pistillata is dominated by tissue-associated Endozoicomonas Bacteria. Appl. Environ. Microbiol. 79, 4759–4762. https://doi.org/10.1128/AEM.00695-13.

Boilard, A., Dubé, C.E., Gruet, C., Mercière, A., Hernandez-Agreda, A., Derome, N., 2020. Defining coral bleaching as a microbial dysbiosis within the coral holobiont. Microorganisms 8, 1682.

Bourne, D.G., Munn, C.B., 2005. Diversity of bacteria associated with the coral *Pocillopora damicornis* from the great barrier reef. Environ. Microbiol. 7, 1162–1174.

Bourne, D.G., Iida, Y., Uthicke, S., Smith-Keune, C., 2008. Changes in coral-associated microbial communities during a bleaching event. ISME J. 2, 350–363.

Bourne, D.G., Dennis, P.G., Uthicke, S., Soo, R.M., Tyson, G.W., Webster, N.S., 2013. Coral invertebrate microbiomes correlate with the presence of photosymbionts. ISME J. 7, 1452–1458.

Bourne, D.G., Morrow, K.M., Webster, N.S., 2016. Insights into the coral microbiome: underpinning the health and resilience of reef ecosystems. Annu. Rev. Microbiol. 70, 317–340.

Brown, A.L., Lipp, E.K., Osenberg, C.W., 2019. Algae dictate multiple stressor effects on coral microbiomes. Coral Reefs 38, 229–240. https://doi.org/10.1007/s00338-019-01769-w.

Ceh, J., Van Keulen, M., Bourne, D.G., 2011. Coral-associated bacterial communities on Ningaloo reef, Western Australia. FEMS Microb. Ecol. 75, 134–144.

Claar, D.C., McDevitt-Irwin, J.M., Garren, M., Vega Thurber, R., Gates, R.D., Baum, J.K., 2020. Increased diversity and concordant shifts in community structure of coral-associated Symbiodiniaceae and bacteria subjected to chronic human disturbance. Mol. Ecol. 29, 2477–2491. https://doi.org/10.1111/mec.15494.

Clarke, K.R., 1993. Nonparametric multivariate analyses of changes in community structure. Aust. Ecol. 18, 117–143. https://doi.org/10.1111/j.1442-9993.1993.tb00438.x.

Clarke, K.R., Gorley, R.N., 2015. PRIMER v7: User Manual/Tutorial. PRIMER-E, Plymouth, United Kingdom.

Clements, C.S., Rasher, D.B., Hoey, A.S., Bonito, V.E., Hay, M.E., 2018. Spatial and temporal limits of coral-macroalgal competition: the negative impacts of macroalgal density, proximity, and history of contact. Mar. Ecol. Prog. Ser. 586, 11–20.

Clements, C.S., Burns, A.S., Stewart, F.J., Hay, M.E., 2020. Seaweed-coral competition in the field: effects on coral growth, photosynthesis and microbiomes require direct contact. Proc. R. Soc. B: Biol. Sci. 287 https://doi.org/10.1098/rspb.2020.0366, 20200366.

Cole, J.R., Wang, Q., Fish, J.A., Chai, B., McGarrell, D.M., Sun, Y., Brown, C.T., Porras-Alfaro, A., Kuske, C.R., Tiedje, J.M., 2014. Ribosomal database project: data and tools for high throughput rRNA analysis. Nucleic Acids Res. 42, D633–D642. https://doi.org/10.1093/nar/gkt1244.

Coolen, M.J.L., Saenz, J.P., Giosan, L., Trowbridge, N.Y., Dimitrov, P., Dimitrov, D., Eglinton, T.I., 2009. DNA and lipid molecular stratigraphic records of haptophyte succession in the Black Sea during the Holocene. Earth Planet. Sci. Lett. 284, 610–621.

Damjanovic, K., Blackall, L.L., Peplow, L.M., Van Oppen, M.J.H., 2020. Assessment of bacterial community composition within and among Acropora loripes colonies in the wildand in captivity. Coral Reefs 39, 1245–1255. https://doi.org/10.1007/s00338-020-01958-y.

De Bakker, D.M., Van Duyl, F.C., Bak, R.P.M., Nugues, M.M., Nieuwland, G., Meesters, E. H., 2017. 40 years of benthic community change on the Caribbean reefs of Curacao and Bonaire: the rise of slimy cyanobacterial mats. Coral Reefs 36, 355–367. https://doi.org/10.1007/s00338-016-1534-9.

De Cáceres, M., Legendre, P., 2009. Associations between species and groups of sites: indices and statistical inference. Ecology 90, 3566–3574.

Diaz, L., 2017. Response of the coral associated nitrogen fixing bacteria toward elevated water temperature. J. Water Resour. Ocean Sci. 6, 98–109. https://doi.org/10.11648/j.wros.20170606.14.

Dubé, C.E., Ziegler, M., Merciere, A., Boissin, E., Planes, S., Bourmaud, C.A.-F., Voolstra, C.R., 2021. Naturally occurring fire coral clones demonstrate a genetic and environmental basis of microbiome composition. Nat. Commun. 12, 6402. https://doi.org/10.1038/s41467-021-26543-x.

Dufrêne, M., Legendre, P., 1997. Species assemblages and indicator species: the need for a flexible asymmetrical approach. Ecol. Monogr. 67, 345–366.

Dunphy, C.M., Gouhier, T.C., Chu, N.D., Vollmer, S.V., 2019. Structure and stability of the coral microbiome in space and time. Sci. Rep. 9, 6785.

Glasl, B., Herndl, G.J., Frade, P., 2016. The microbiome of coral surface mucus has a key role in mediating holobiont health and survival upon disturbance. ISME J. 10, 2280–2292. https://doi.org/10.1038/ismej.2016.9.

Gleason, M., 1993. Effects of disturbance on coral communities: bleaching in Moorea, French Polynesia. Coral Reefs 12, 193–201.

Glynn, P.W., D'Croz, L., 1990. Experimental evidence for high temperature stress as the cause of El Niño-coincident coral mortality. Coral Reefs 8, 181–191.

Haas, A.F., Gregg, A.K., Smith, J.E., Abieri, M.L., Hatay, M., Rohwer, F., 2013. Visualization of oxygen distribution patterns caused by coral and algae. PeerJ 1, e106. https://doi.org/10.7717/peerj.106.

Hernandez-Agreda, A., Leggat, W., Bongaerts, P., Herrera, C., Ainsworth, T.D., 2018. Rethinking the coral microbiome: simplicity exists within a diverse microbial biosphere. mBio 9 e00812–00818.

Hueerkamp, C., Glynn, P.W., D'Croz, L., Maté, J.L., Colley, S.B., 2001. Bleaching and recovery of five eastern Pacific corals in an El Nino-related temperature experiment. Bull. Mar. Sci. 69, 215–236.

Huggett, M., Apprill, A., 2019. Coral microbiome database: integration of sequences reveals high diversity and relatedness of coralassociated microbes. Environ. Microbiol. Rep. 11, 372–385. https://doi.org/10.1111/1758-2229.12686.

Jackson, J., Donavan, M., Cramer, K., Lam, V., 2014. Status and Trends of Caribbean Coral Reefs: 1970–2012. CEP Technical Report. IUCN, UNEP, p. 303.

Johnston, I.S., Rohwer, F., 2007. Microbial landscapes on the outer tissue surfaces of the reef-building coral *Porites compressa*. Coral Reefs 26, 375–383.

Jones, R.J., Yellowlees, D., 1997. Regulation and control of intracellular algae (=zooxanthellae) in hard corals. Phil. Trans. R. Soc. London 352B, 457–468.

Jones, R.J., Hoegh-Guldberg, O., Larkum, A.W.D., Schreiber, U., 1998. Temperature-induced bleaching of corals begins with impairment of the CO2 fixation mechanism in zooxanthellae. Plant, Cell Env. 21, 1219–1230.

Kelly, L.W., Williams, G.J., Barott, K.L., Carlson, C.A., Dinsdale, E.A., Edwards, R.A., Haas, A.F., Haynes, M., Lim, Y.W., McDole, T., Nelson, C.E., Sala, E., Sandin, S.A., Smith, J.E., Vermeij, M.J.A., Youle, M., Rohwer, F., 2014. Local genomic adaptation of coral reef-associated microbiomes to gradients of natural variability and anthropogenic stressors. Proc. Natl. Acad. Sci. 111, 10227–10232.

Klaus, J.S., Janse, I., Heikoop, J.M., Santford, R.A., Fouke, B.W., 2007. Coral microbial communities, zooxanthellae and mucus along gradients of seawater depth and coastal pollution. Environ. Microbiol. 9, 1291–1305.

Klindworth, A., Pruesse, R., Schweer, T., Peplies, J., Quast, C., Horn, M., Glöckner, F., 2013. Evaluation of general 16S ribosomal RNA gene PCR primers for classical and next-generation sequencing-based diversity studies. Nucleic Acids Res. 41, e1.

Krediet, C.J., Ritchie, K.B., Paul, V.J., Teplitski, M., 2013. Coral-associated micro-organisms and their role in promoting coral health and thwarting diseases. Proc. R. Soc. B 280. https://doi.org/10.1098/rspb.2012.2328, 201222328.

Kvennefors, E.C.E., Sampayo, E., Kerr, C., Vieira, G., Roff, G., Barnes, A.C., 2011. Regulation of bacterial communities through antimicrobial activity of the coral holobiont. Microb. Ecol. 63, 605–618. https://doi.org/10.1007/s00248-011-9946-0.

Lang, J., Lasker, H., Gladfelter, E., Hallock, P., 1992. Spatial and temporal variability during periods of "recovery" after mass bleaching on Western Atlantic coral reefs. Am. Zool. 32, 696–706. https://doi.org/10.1093/icb/32.6.696.

Maher, R.L., Schmeltzer, E.R., Meiling, S., McMinds, R., Ezzat, L., Shantz, A.A., Adam, T. C., Schmitt, R.J., Sj, Holbrook, Burkepile, D.E., Vega, Thurber R., 2020. Coral microbiomes demonstrate flexibility and resilience through a reduction in community diversity following a thermal stress event. Front. Ecol. Evol. 15 https://doi.org/10.3389/fevo.2020.555698.

Mahmoud, H.M., Kalendar, A.A., 2016. Coral-associated Actinobacteria: diversity, abundance, and biotechnological potentials. Front. Microbiol. 7, 204. https://doi.org/10.3389/fmicb.2016.00204.

Mao-Jones, J., Ritchie, K.B., Jones, L.E., Ellner, S.P., 2010. How microbial community composition regulates coral disease development. PLoS Biol. 8 e1000345.

McCook, L.J., Jompa, J., Diaz-Pulido, G., 2001. Competition between corals and algae on coral reefs: a review of evidence and mechanisms. Coral Reefs 19, 400–417.

McDevitt-Irwin, J.M., Baum, J.K., Garren, M., Vega Thurber, R.L., 2017. Responses of coral-associated bacterial communities to local and global stressors. Front. Mar. Sci. 4, 262. https://doi.org/10.3389/fmars.2017.00262.

Morrow, K.M., Paul, V.J., Liles, M.R., Chadwick, N.E., 2011. Allelochemicals produced by Caribbean macroalgae and cyanobacteria have species-specific effects on reef coral microorganisms. Coral Reefs 30, 309–320.

Morrow, K.M., Rl, Ritson-Williams, Ross, C., Liles, M.R., Paul, V.J., 2012. Macroalgal extracts induce bacterial assemblage shifts and sublethal tissue stress in Caribbean corals. PlosOne 7 e44859.

Morrow, K.M., Liles, M.R., Paul, V.J., Moss, A.G., Chadwick, N.E., 2013. Bacterial shifts associated with coral-macroalgal competition in the Caribbean Sea. Mar. Ecol. Prog. Ser. 488, 103–117.

Mouchka, M.E., Hewson, I., Harvell, C.D., 2010. Coral-associated bacterial assemblages: current knowledge and the potential for climate-driven impacts. Integr. Comp. Biol. 50, 662–674.

Mueller, B., van der Zande, R., van Leent, P., Meesters, E., Vermeij, M., van Duyl, F., 2014. Effect of light availability on dissolved organic carbon (DOC) release by Caribbean reef algae and corals. Bull. Mar. Sci. 90, 875–893.

Neave, M.J., Apprill, A., Ferrier-Pagès, C., Voolstra, C.R., 2016. Diversity and function of prevalent symbiotic marine bacteria in the genus Endozoicomonas. Appl. Microbiol. Biotechnol. 100, 8315–8324. https://doi.org/10.1007/s00253-016-7777-0.

Nelson, C.E., Goldberg, S.J., Wegley Kelly, L., Haas, A.F., Smith, J.E., Rohwer, F., Carlson, C.A., 2013. Coral and macroalgal exudates vary in neutral sugar composition and differentially enrich reef bacterioplankton lineages. ISME J. 7, 962–979.

Nugues, M.M., Bak, R.P.M., 2009. Brown-band syndrome on feeding scars of the crown-of-thorn starfish *Acanthaster planci*. Coral Reefs 28, 507–510.

Nugues, M.M., Szmant, A.M., 2006. Coral settlement onto *Halimeda opuntia* : a fatal attraction to an ephemeral substrate? Coral Reefs 25, 585–591. https://doi.org/10.1007/s00338-006-0147-0.

Nugues, M.M., Smith, G.W., Van Hooidonk, R.J., Seabra, M.I., Bak, R.P.M., 2004. Algal contact as a trigger for coral disease. Ecol. Lett. 7, 919–923.

Obura, D.O., 2009. Reef corals bleach to resist stress. Mar. Pollut. Bull. 58, 206–212.

Parwati, E., Kartasasmita, M., Soewardi, K., Kusumastanto, T., Nurjaya, I.W., 2013. The relationship between total suspended solids (TSS) and coral reef growth (case study of Derawan Island, Delta Berau waters). Int. J. Remote Sens. Earth Sci. 10, 104–113. https://doi.org/10.30536/j.ijreses.2013.v10.a1849.

Peixoto, R.S., Rosado, P.M., Leite, DcdA, Rosado, A.S., Bourne, D.G., 2017. Beneficial microorganisms for corals (BMC): proposed mechanisms for coral health and resilience. Front. Microbiol. 8 (2017), 00341. https://doi.org/10.3389/fmicb.2017.00341.

Pootakham, W., Mhuantong, W., Yoocha, T., Putchim, L., Sonthirod, C., Naktang, C., Thongtham, N., Tangphatsornruang, S., 2017. High resolution profiling of coral associated bacterial communities using full-length 16S rRNA sequence data from PacBio SMRT sequencing system. Sci. Rep. 7, 2774. https://doi.org/10.1038/s41598-017-03139-4.

Rasher, D.B., Hay, M.E., 2010. Chemically rich seaweeds poison corals when not controlled by herbivores. Proc. Nat. Acad. Sci. USA (PNAS) 107, 9683–9688.

Ritchie, K.B., 2006. Regulation of microbial populations by coral surface mucus and mucus-associated bacteria. Mar. Ecol. Prog. Ser. 322, 1–14.

Ritchie, K.B., Smith, G.W., 2004. Microbial communities of coral surface mucopolysaccharide layers. In: YL, E. Rosenberg (Ed.), Coral Health and Disease. Springer, Berlin.

Roach, T.N.F., Little, M., Arts, M.G.I., Huckeba, J., Haas, A.F., George, E.E., Quinn, R.A., Cobián-Güemes, A.G., Naliboff, D.S., Silveira, C.B., Vermeij, M.J.A., Kelly, L.W., Dorrestein, P.C., Rohwer, F., 2020. A multiomic analysis of in situ coral–turf algal interactions. PNAS 117, 13588–13595.

Rodríguez-Román, A., Hernández-Pech, X., Thomé, P.E., Enríquez, S., Iglesias-Prieto, R., 2006. Photosynthesis and light utilization in the Caribbean coral Montastraea faveolata recovering from a bleaching event. Limnol. Oceanogr. 51, 2702–2710.

Rosales, S.M., Clark, A.S., Huebner, L.K., Ruzicka, R.R., Muller, E.M., 2020. Rhodobacterales and rhizobiales are associated with stony coral tissue loss disease and its suspected sources of transmission. Front. Microbiol. 11, 681. https://doi.org/10.3389/fmicb.2020.00681.

Rosenberg, E., Koren, O., Reshef, L., Efrony, R., Zilber-Rosenberg, I., 2007. The role of microorganisms in coral health, disease and evolution. Nat. Rev. Microbiol. 5, 355–362.

Rosenberg, E., Kushmaro, A., Kramarsky-Winter, E., Banin, E., Yossi, L., 2009. The role of microorganisms in coral bleaching. ISME J. 3, 139–146. https://doi.org/10.1038/ismej.2008.104.

Rypien, K.L., Ward, J.R., Azam, F., 2009. Antagonistic interactions among coral-associated bacteria. Environ. Microbiol. 12, 28–39.

Shearer, T.L., Rasher, D.B., Snell, T.W., Hay, M.E., 2012. Gene expression patterns of the coral Acropora millepora in response to contact with macroalgae. Coral Reefs 31, 1177–1192.

Smith, J.E., Shaw, M., Edwards, R.A., Obura, D., Pantos, O., Sala, E., Sandin, S.A., Smriga, S., Hatay, M., Rohwer, F.L., 2006. Indirect effects of algae on coral: algae-mediated, microbe-induced coral mortality. Ecol. Lett. 9, 835–845.

Sunagawa, S., Woodley, C., Medina, M., 2010. Threatened corals provide underexplored microbial habitats. PlosOne 5. https://doi.org/10.1371/journal.pone.0009554 e9554.

Sweet, M.J., Croquer, A., Bythell, J.C., 2011. Dynamics of bacterial community development in the reef coral Acropora muricata following experimental antibiotic treatment. Coral Reefs 30, 1121–1133.

Sweet, M.J., Bythell, J.C., Nugues, M.M., 2013. Algae as reservoir for coral pathogens. PlosOne 8, e69717.

Taruttis, F., Spang, R., Engelmann, J.C., 2015. A statistical approach to virtual cellular experiments: improved causal discovery using accumulation IDA (aIDA). Bioinformatics 31, 3807–3814. https://doi.org/10.1093/bioinformatics/btv461.

Titlyanov, E.A., Yakovleva, I.I., Titlyanova, T.V., 2007. Interaction between benthic algae (*Lyngbya bouilonii*, *Dictyota dichtoma*) and scleractinian coral *Porites lutea* in direct contact. J. Exp. Mar. Biol. Ecol. 342, 282–291.

Vega Thurber, R., Willner-Hall, D., Rodriguez-Mueller, B., Desnues, C., Edwards, R.A., Angly, F., Dinsdale, E.A., Kelly, L., Rohwer, F., 2009. Metagenomic analysis of stressed coral holobionts. Environ. Microbiol. 11, 2148–2163.

Vega Thurber, R., Burkepile, D.E., Correa, A.M.S., Thurber, A.R., Shantz, A.A., Welsh, R., Pritchard, C., Rosales, S., 2012. Macroalgae decrease growth and alter microbial community structure of the reef-building coral, *Porites astreoides*. PlosOne 7 e44246.

Voolstra, C.R., Ziegler, M., 2020. Adapting with microbial help: microbiome flexibility facilitates rapid responses to environmental change. BioEssays 42, 9. https://doi.org/10.1002/bies.202000004.

Waite, D.W., Chuvochina, M., Pelikan, C., Parks, D.H., Yilmaz, P., Wagner, M., Loy, A., Naganuma, T., Nakai, R., Whitman, W.B., Hahn, M.W., Kuever, J., Hugenholtz, P., 2020. Proposal to reclassify the proteobacterial classes Deltaproteobacteria and Oligoflexia, and the phylum Thermodesulfobacteria into four phyla reflecting major functional capabilities. Int. J. Syst. Evol. Microbiol. 70, 5972–6016. https://doi.org/10.1099/ijsem.0.004213.

Wangpraseurt, D., Weber, M., Roy, H., Polerecky, L., De Beer, D., Suharsono, Nugues, M. M., 2012. In situ oxygen dynamics in coral-algal interactions. PlosOne 7 e31192.

Welsh, R.M., Zaneveld, J.R., Rosales, S.M., Payet, J.P., Burkepile, D.E., Vega Thurber, R. L., 2016. Bacterial predation in a marine host-associated microbiome. ISME J. 10, 1540–1544. https://doi.org/10.1038/ismej.2015.219.

Welsh, R.M., Rosales, S.M., Zaneveld, J.R., Payet, J.P., McMinds, R., Hubbs, S.L., Vega Thurber, R.L., 2017. Alien vs. predator: bacterial challenge alters coral microbiomes unless controlled by Halobacteriovorax predators. PeerJ 5. https://doi.org/10.7717/peerj.3315 e3315.

Williams, A.D., Brown, B.E., Putchim, L., Sweet, M.J., 2015. Age-related shifts in bacterial diversity in a reef coral. PLoS One 10, e0144902. https://doi.org/10.1371/journal.pone.0144902.

Wooldridge, S.A., 2013. Breakdown of the coral-algae symbiosis: towards formalising a linkage between warm-water bleaching thresholds and the growth rate of the intracellular zooxanthellae. Biogeosciences 10, 1647–1658. https://doi.org/10.5194/bg-10-1647-2013.

Wuchter, C., Schouten, S., Coolen, M.J.L., Sinninghe-Damste, J., 2004. Temperature-dependent variation in the distribution of tetraether membrane lipids of marine Crenarchaeota: implications for TEX 86 paleothermometry. Paleoceanography 19, 4028. https://doi.org/10.1029/2004PA001041.

Wuchter, C., Banning, E., Mincer, T., Drenzek, N.J., Coolen, M.J.L., 2013. Microbial diversity and methanogenic activity of Antrim shale formation waters from recently fractured wells. Front. Microbiol. 4, 1–20 (plus supplementary information).

Yilmaz, P., Wegener Parfrey, L., Yarza, P., Gerken, J., Pruesse, E., Quast, C., Schweer, T., Peplies, J., Ludwig, W., Glöckner, F., 2014. The SILVA and "All-species Living Tree Project (LTP)" taxonomic frameworks. Nucleic Acids Res. 42 https://doi.org/10.1093/nar/gkt1209.

Zaneveld, J.R., Burkepile, D.E., Shantz, A.A., Pritchard, C.E., McMinds, R., Payet, J.P., Welsh, R., Correa, A.M.S., Lemoine, N.P., Rosales, S., Fuchs, C., Maynard, J.A., Thurber, R.V., 2016. Overfishing and nutrient pollution interact with temperature to disrupt coral reefs down to microbial scales. Nat. Commun. 7, 11833. https://doi.org/10.1038/nscomms11833.

Ziegler, M., Grupstra, C.G.B., Barreto, M.M., Eaton, M., BaOmar, J., Zubier, K., Al-Sofyani, A., Turki, A.J., Ormond, R., Voolstra, C.R., 2019. Coral bacterial community structure responds to environmental change in a host-specific manner. Nat. Commun. https://doi.org/10.1038/s41467-019-10969-5.